

NASA Technical Memorandum 83208

NASA-TM-83208 19820005174

Wind-Tunnel Investigation of the Tail-Spoiler Concept for Stall Prevention on General Aviation Airplanes

Dale R. Satran

NOVEMBER 1981

FOR RELEASE
ON 11-11-81
NASA-83208

NASA

NASA Technical Memorandum 83208

Wind-Tunnel Investigation of the Tail-Spoiler Concept for Stall Prevention on General Aviation Airplanes

Dale R. Satran
Langley Research Center
Hampton, Virginia



National Aeronautics
and Space Administration

**Scientific and Technical
Information Branch**

1981

INTRODUCTION

NASA Langley Research Center is currently conducting an intensive research program on the stall/spin characteristics of small general aviation aircraft. The stall/spin problem is being studied because in recent years, over 28 percent of the fatal general aviation accidents have been related to stall/spin problems (refs. 1 and 2). In this program, several aerodynamic and control system concepts are being studied as possible solutions to the stall/spin problem. These include wing modifications, tail configuration changes, fuselage cross-sectional changes, and active stall-prevention control systems (refs. 3 through 6).

The concept of preventing airplane stall by limiting pitch-control power was demonstrated 40 years ago by airplanes such as the Erco Ercoupe and the General Skyfarer (ref. 7). This particular approach, which utilized elevator travel limits, has proven to be technically unfeasible for today's designs, which typically exhibit larger flap and power effects and a wide range of center-of-gravity travel.

In recent years, H. L. Chevalier at Texas A & M University developed an active stall-prevention system to accommodate these variables. The system uses angle-of-attack feedback information to automatically deflect an antistall control surface (an aerodynamic tail spoiler) as shown in figure 1. Deflection of the spoiler produces a nose-down moment which limits the nose-up trim capability of the elevator to an angle of attack below the stall angle (see fig. 2). The system provides a trim point, $C_m = 0$, that is below the stall angle of attack by a margin of 1° or 2° , as illustrated in figure 3. The tail-spoiler concept also increases the longitudinal stability and elevator hinge moments of the aircraft as the stall is approached (ref. 8).

Earlier research, which included flight tests with single- and twin-engine airplanes (refs. 9 and 10), demonstrated the feasibility of the concept; however, no aerodynamic data were available for analysis or design purposes. The investigation presented herein was conducted in the Langley 30- by 60-Foot Wind Tunnel on a full-scale powered model to evaluate the static aerodynamic effects of this concept and to provide information on Reynolds number effects to complete the work begun in reference 8. The effects of various tail-spoiler deflections were measured for several elevator deflections, power settings, and flap deflections.

SYMBOLS

The longitudinal forces and moments are referred to the stability-axis system (shown in fig. 4) and are referenced, unless otherwise noted, to a center-of-gravity position which corresponds to 25 percent of the mean aerodynamic chord. All measurements and calculations were made in U.S. Customary Units; however, dimensional quantities have been presented both in the International System of Units (SI) and parenthetically in U.S. Customary Units. Conversion factors for the two systems are found in reference 11.

C_D drag coefficient, $\text{Drag}/q_\infty S$

C_{he} elevator hinge-moment coefficient, $M_{he}/q_\infty S_e \bar{c}_e$

C_L	lift coefficient, $Lift/q_\infty S$
C_m	pitching-moment coefficient, $Pitching\ moment/q_\infty S \bar{c}$
$C_{m\delta_e}$	pitching-moment coefficient due to elevator deflection (elevator effectiveness), per deg
$C_{T'}$	effective thrust coefficient, $T'/q_\infty S$
\bar{c}	wing mean aerodynamic chord, m (ft)
\bar{c}_e	elevator mean aerodynamic chord, m (ft)
\bar{c}_t	horizontal-tail mean aerodynamic chord, m (ft)
D	propeller diameter, m (ft)
h	projected vertical height of deflected tail spoiler, m (ft)
J	propeller advance ratio, V/nD
M_{he}	elevator hinge moment, positive when hinge moment tends to deflect control surface in a positive direction
n	propeller rotational speed, rps
q_∞	free-stream dynamic pressure, $\rho V^2/2$, Pa (lbf/ft ²)
R	Reynolds number, $\rho V \bar{c} / \mu$
S	wing area, m ² (ft ²)
S_e	elevator area, m ² (ft ²)
T'	effective thrust at $\alpha = 0^\circ$, drag with propeller removed minus drag with propeller operating, N (lbf)
V	free-stream velocity, m/s (ft/s)
X_s, Y_s, Z_s	stability axes
α	angle of attack (referenced to airplane longitudinal axis, see fig. 4), deg
δ_e	elevator-deflection angle, positive trailing edge down, deg
δ_f	flap-deflection angle, positive trailing edge down, deg
δ_{sp}	spoiler-deflection angle, positive trailing edge down, deg
$\Delta\alpha$	incremental angle of attack, deg
μ	viscosity of air, Pa-s (slugs/ft-s)
ρ	mass density of air, kg/m ³ (slugs/ft ³)

Subscripts:

a spoiler deployment

max maximum

s stall

Abbreviations:

AOA angle of attack

c.g. center of gravity

EXPERIMENTAL PROCEDURE

Wind Tunnel

The Langley 30- by 60-Foot Wind Tunnel (ref. 12) is an open-throat, double-return atmospheric tunnel which can be operated at dynamic pressures from 50 to 1440 Pa (1 to 30 lbf/ft²). The test section is 9 m (30 ft) high by 18 m (60 ft) wide. Full-scale models are typically attached to an external set of scales by a three-strut mounting arrangement. The forces and moments produced by the model are resolved from strain gage outputs of the scales.

Model

The low-wing single-engine general aviation model used in this investigation is the same full-scale model used in reference 13 except that the incidence of the horizontal stabilizer was set to 0° and the elevator was notched. Table I and figure 5 give the principal dimensions of the model. A photograph of the model in the Langley 30- by 60-Foot Wind Tunnel is shown in figure 6. Control surfaces, which were remotely controlled, consisted of ailerons, rudder, elevator, and plain unsealed flaps.

Tail Spoiler

A previous wind-tunnel study with an isolated full-scale horizontal tail and tail spoiler determined that the most effective chordwise location for the tail spoiler is at the hinge line of the elevator or at the 75 percent chord of a stabilator.

For this investigation, a full-span spoiler was mounted with a piano hinge on the lower surface of the horizontal stabilizer near the hinge line of the elevator. As shown in figure 7, the tail spoiler when fully retracted created a 0.64 cm (0.25 in.) discontinuity along the lower surface of the horizontal stabilizer. The trailing edge of the spoiler ended flush with the trailing edge of the horizontal stabilizer. The spoiler had a constant 5.08 cm (2.0 in.) chord and could be deflected up to 90° ($h/\bar{c}_t = 0.0605$).

Instrumentation

During the investigation, a data acquisition system recorded the aerodynamic forces and moments and instrumentation outputs on magnetic tape. The positions of the control surfaces were measured with potentiometers, and the torque tube of the elevator was instrumented with strain gages to measure the hinge moment of the elevator. Angle of attack was measured with a calibrated accelerometer mounted inside the model. A pressure transducer, thermocouple, barometer, and hygrometer were used to determine the air density and velocity of the tests.

Tests and Methods

The tests were conducted at free-stream dynamic pressures of 407 Pa (8.5 lbf/ft²) and 479 Pa (10.0 lbf/ft²) which provided test velocities of 26 m/s (86 ft/s) and 29 m/s (95 ft/s), respectively. These velocities, in combination with the appropriate engine speeds, were used to provide the propeller advance ratios for cruise ($J = 0.63$) and climb ($J = 0.45$) flight conditions. Unless otherwise noted, the Reynolds number R based on the wing mean aerodynamic chord and average test velocity was 2.3×10^6 , which was representative of the full-scale airplane at landing conditions.

The spoiler was evaluated for four flight conditions: power off (propeller windmilling or $C_{T_i} = -0.01$ and $\delta_f = 0^\circ$), cruise ($C_{T_i} = 0.09$ and $\delta_f = 0^\circ$), approach ($C_{T_i} = 0.09$ and $\delta_f = 30^\circ$), and go-around (full power or $C_{T_i} = 0.25$ and $\delta_f = 30^\circ$). The power effects have not been removed from the data presented.

The longitudinal data from these tests have been corrected for blockage, air-stream misalignment, buoyancy effects, mounting strut tares including propeller slipstream effects, and wind-tunnel jet boundary effects on both wing and tail. Propeller slipstream effects at the tail are also accounted for in the tail-on jet boundary corrections. The corrections to the data were insignificant for this investigation.

Operationally, the tail spoiler is designed to be deflected as a nonlinear function of changes in angle of attack. The spoiler deployment schedule, shown in figure 8, is defined by the following equation:

$$h/\bar{c}_t = 2.17 \times 10^{-3} (\Delta\alpha)^{2.4}$$

where $\Delta\alpha = \alpha - \alpha_a$ ($0 < \Delta\alpha < 4$) and $\alpha_s - \alpha_a = 4^\circ$. The nondimensional ratio h/\bar{c}_t is used in presenting the data, although figure 8 also shows the relationship of h/\bar{c}_t to δ_{sp} . As noted in the description of the tail spoiler, there was a zero offset between h/\bar{c}_t and δ_{sp} . The angle-of-attack range for deployment and the spoiler deployment schedule reflect the refinements in recent studies (refs. 8 and 14). The spoiler deployment schedule is designed to provide smooth transition from the basic pitching-moment characteristics.

For this investigation, the tail spoiler was tested without the output of an angle-of-attack sensor. For fixed spoiler deflections, the model was tested through angles of attack from 0° to 20° . The tail-spoiler data presented are the result of several angle-of-attack sweeps for different spoiler deflections. The spoiler

deployment schedule shown in figure 8 was used to determine the appropriate data points that would illustrate an operational system. Tuft studies were used to determine the airflow over the horizontal tail.

RESULTS AND DISCUSSION

Model Without Tail Spoiler

Longitudinal characteristics.- Shown in figure 9 are the longitudinal characteristics of the model for the four flight conditions investigated. The stall angle of attack (α for $C_{L,max}$) for the model with power off and flaps retracted was about 11° . With power on and/or flaps deflected, the stall angle of attack was at or above 12° .

As shown in figure 10, the amount of elevator travel available allowed the model to be trimmed above the stall angle of attack; therefore, a stall-prevention device would be needed. Deflection of the elevator did not affect the stall angle of attack nor the stability of the model. If a stall-prevention system is to be installed on the model, the angle-of-attack margin for the model to remain below the stall must be defined. It was expected that preventing the model from being trimmed at $\alpha = 11^\circ$ would permit sufficient safety of operation for the flaps-down, power-on conditions as well as for the flaps-up, power-off condition. With the angle of attack limited to 11° , the angle-of-attack margin is less than 2° for the higher power settings and about 0° for the power-off condition.

Note that many pilots limit their airplanes by even larger margins to avoid a stall (ref. 15). With a stall-prevention system on their airplanes, these pilots could safely utilize most of the airplanes' lifting capabilities.

Effects of Reynolds number.- The effects of changes in Reynolds number are shown in figure 11. The principal difference due to Reynolds number is the change of several degrees in the stall angle of attack. To design the tail-spoiler system correctly for the maximum available angle of attack, tests should be performed at the correct Reynolds number.

Model With Tail Spoiler

Effects of tail-spoiler installation.- The effects of the installation of the tail spoiler are shown in figure 12. Figure 12(a) shows that there was a trim change; but the undeflected tail spoiler had no other effects on the longitudinal characteristics of the model. During the investigation, tuft studies were conducted to show the flow over the lower surface of the horizontal tail. Figure 12(b) shows the attached flow on the elevator without the tail spoiler. As shown in figure 12(c), the airflow over the elevator with the spoiler was separated even with the spoiler and elevator undeflected and the angle of attack at 0° . The tail spoiler, as mentioned in the model description, created a discontinuity on the lower surface of the horizontal tail, which caused the flow to separate. The separated flow reduced the contribution of the horizontal tail and caused the change in trim. In figures 12(d) and 12(e), the expanded drag polars show the increase in drag due to the flow separation. At a lift coefficient of 0.4, the increase in drag due to the spoiler was estimated to give a cruise penalty of 0.44 m/s (1 mph) or less while at a lift coefficient of 0.7, the drag due to the spoiler resulted in a climb penalty of

0.14 m/s (27 ft/min). These results indicate that the tail spoiler should be installed so that it retracts flush with the horizontal-tail lower surface.

Spoiler effectiveness.- The results of tests to determine the spoiler effectiveness are presented in figure 13 for $\alpha = 10.5^\circ$. The data are presented at $\alpha = 10.5^\circ$ because this angle of attack is the closest measured angle of attack to the stall angle of 11° . The data of figure 13 show that the variation of pitching moment with tail-spoiler deflection was essentially linear over the range of values of h/c_t from 0.02 to 0.04. For elevator deflections between 0° and -15° , the spoiler generally lost effectiveness below values of $h/\bar{c}_t = 0.02$. However, for large elevator deflections, the spoiler was very effective at low values of h/\bar{c}_t . The spoiler effectiveness generally decreased as the spoiler deflection was increased above a value of h/\bar{c}_t of 0.04.

The cruise condition (fig. 13(b)) and go-around condition (fig. 13(d)) require the largest spoiler deflections for trim at $\alpha = 10.5^\circ$ with full-up elevator deflection ($\delta_e = 23^\circ$); consequently, these two flight conditions are considered the most critical conditions for prevention of model stall. For example, the data show that the cruise and go-around conditions require values of h/\bar{c}_t of 0.035 and 0.04, respectively, for trim with full-up elevator. Therefore, the subsequent analysis of the spoiler effectiveness is limited to these two critical flight conditions.

Elevator effectiveness.- Figure 14 shows the data from figure 13 plotted against elevator deflection for various tail-spoiler deflections for the cruise and go-around flight conditions. The data of figure 14 show that the elevator effectiveness $C_{m\delta_e}$

for elevator deflections from -15° to 0° was reduced for all tail-spoiler deflections. However, the reduction in elevator effectiveness occurred as soon as the tail spoiler was deflected and then generally remained unchanged for greater spoiler deflections. The elevator effectiveness of the model is shown in figure 15 for the cruise and go-around flight conditions. The data show that the elevator effectiveness was reduced after the spoiler was deflected.

Operational tail spoiler simulated.- As described in "Tests and Methods," the tail spoiler was tested without the output of an angle-of-attack sensor. The tail-spoiler data presented are the result of several angle-of-attack sweeps for different spoiler deflections. The tail spoiler was effective over the entire angle-of-attack range tested, regardless of whether the horizontal tail was providing an up load or down load.

The pitching-moment characteristics of the model with an operational tail spoiler simulated for the cruise and go-around conditions are shown in figure 16. The tail spoiler limited the trim angle of attack for all elevator deflections to below the stall-margin-limited angle of attack ($\alpha = 11^\circ$). The tail spoiler also produced a nose-down pitching-moment change with angle of attack which increased the static stability of the model as shown.

Presented in figure 17 is elevator hinge moment coefficient with the tail spoiler deflected. There was an increase in the elevator hinge moment with spoiler deflection. The increase in the hinge moment would produce an increase in the stick force for the pilot as the airplane approached the stall.

Effects of center-of-gravity position.- Shown in figure 18 are the pitching-moment characteristics of the model with an operational tail spoiler simulated for the go-around condition with the c.g. at the aft limit of $0.271\bar{c}$, and for the cruise

condition with the c.g. at the forward limit of 0.219C. The go-around, aft c.g. condition was the more difficult condition from which to prevent the model from being trimmed above the limit of $\alpha = 11^\circ$. As shown in figure 18(a), the tail spoiler limited the trim angle of attack of the airplane to 11° against full elevator deflection. As shown in figure 18(b), the forward c.g., cruise condition was the easier condition to prevent model stall. The tail spoiler limited the trim angle of attack to 10° against full elevator deflection. This reduced trim angle of attack represented a 4 percent reduction in maximum lift available for the cruise condition.

CONCLUDING REMARKS

Active stall-prevention systems, such as the tail-spoiler concept, must be designed to accommodate large flap and power effects and a wide range of center-of-gravity (c.g.) positions. The tail-spoiler system was shown to be capable of preventing the model from being trimmed above the stall because it provides a nose-down pitching moment at the stall. The tail spoiler increased the longitudinal stability and elevator hinge moment near the stall. The tail spoiler was effective over the entire angle-of-attack range tested, regardless of whether the horizontal tail was providing an up load or a down load.

For configurations with more effective flap systems, such as slotted or Fowler flaps, the stall angle of attack may shift several degrees because of flap deflection. The angle of attack for tail-spoiler deployment may need to be a function of flap deflection to avoid large losses in available lift. Similar refinements may be required for airplanes with large power effects or a wide c.g. range, particularly for high-wing airplanes. Finally, there is a need to investigate ground effects and dynamic effects such as accelerated stalls.

For the low-wing, single-engine model tested, the effects of flaps, power, and c.g. position are small and additional refinements may not be needed.

Langley Research Center
National Aeronautics and Space Administration
Hampton, VA 23665
September 28, 1981

REFERENCES

1. Silver, Brent W.: Statistical Analysis of General Aviation Stall Spin Accidents. [Preprint] 760480, Soc. Automat. Eng., Apr. 1976.
2. Ellis, David R.: A Study of Lightplane Stall Avoidance and Suppression. FAA-RD-77-25, Feb. 1977.
3. Staff of Langley Research Center: Exploratory Study of the Effects of Wing-Leading-Edge Modifications on the Stall/Spin Behavior of a Light General Aviation Airplane. NASA TP-1589, 1979.
4. Burk, Sanger M., Jr.; Bowman, James S., Jr.; and White, William L.: Spin-Tunnel Investigation of the Spinning Characteristics of Typical Single-Engine General Aviation Airplane Designs. I - Low-Wing Model A: Effects of Tail Configurations. NASA TP-1009, 1977.
5. Bennett, A. G.; Owens, J. K.; and Bull, G.: A Study of Stall Deterrent Systems for General Aviation Aircraft. A Collection of Technical Papers - AIAA Atmospheric Flight Mechanics Conference, Aug. 1980, pp. 51-61. (Available as AIAA-80-1562.)
6. Chevalier, Howard L.; Brown, Jeff R.; and Wilke, Robert A.: A Method for Preventing Airplane Stall/Spin. AIAA Paper 74-863, Aug. 1974.
7. Chambers, Joseph R.: Overview of Stall/Spin Technology. AIAA-80-1580, Aug. 1980.
8. Chevalier, H. L.: Some Theoretical Considerations of a Stall Proof Airplane. [Preprint] 790604, Soc. Automat. Eng., Apr. 1979.
9. Chevalier, Howard; and Brusse, Joseph C.: A Stall/Spin Prevention Device for General-Aviation Aircraft. [Preprint] 730333, Soc. Automat. Eng., Apr. 1973.
10. Chevalier, H. L.: Aerodynamic Spoiler for Preventing Airplane Stall/Spin Type Accidents. FAA-RD-75-21, Dec. 1974.
11. Standard for Metric Practice: E 380-79, American Soc. Testing & Mater., c.1980.
12. DeFrance, Smith J.: The N.A.C.A. Full-Scale Wind Tunnel. NACA Rept. 459, 1933.
13. Johnson, Joseph L., Jr.; Newsom, William A., Jr.; and Satran, Dale R.: Full-Scale Wind-Tunnel Investigation of the Effects of Wing Leading-Edge Modifications on the High Angle-of-Attack Aerodynamic Characteristics Of a Low-Wing General Aviation Airplane. AIAA-80-1844, Aug. 1980.
14. Chevalier, H. L.; and Faulkner, M. L.: Full-Scale Test of a Stall Proof Device. AIAA-80-1899, Aug. 1980.
15. Goode, Maxwell W.; O'Bryan, Thomas C.; Yenni, Kenneth R.; Cannaday, Robert L.; and Mayo, Marna H.: Landing Practices of General Aviation Pilots in Single-Engine Light Airplanes. NASA TN D-8283, 1976.

TABLE I.- TEST AIRPLANE DIMENSIONAL CHARACTERISTICS

Center of gravity, percent \bar{c}	25
Wing:	
Span, m (ft)	7.46 (24.46)
Area, m ² (ft ²)	9.11 (98.11)
Root chord, m (ft)	1.22 (4.0)
Tip chord, m (ft)	1.22 (4.0)
Mean aerodynamic chord, m (ft)	1.22 (4.0)
Aspect ratio	6.10
Dihedral, deg	5.0
Incidence:	
At root, deg	3.5
At tip, deg	3.5
Airfoil	NACA 64 ₂ -415 (modified by removing trailing-edge reflex)
Flaps:	
Span, m (ft)	1.22 (4.01)
Area, each, m ² (ft ²)	0.25 (2.72)
Mean aerodynamic chord, m (ft)	0.21 (0.68)
Hinge line, percent \bar{c}	85.4
Ailerons:	
Span, m (ft)	1.16 (3.81)
Area, each, m ² (ft ²)	0.24 (2.60)
Mean aerodynamic chord, m (ft)	0.20 (0.65)
Hinge line, percent \bar{c}	85.4
Vertical tail:	
Span, m (ft)	1.17 (3.85)
Area, m ² (ft ²)	0.78 (8.37)
Root chord, m (ft)	1.10 (3.60)
Tip chord, m (ft)	0.51 (1.67)
Mean aerodynamic chord, m (ft)	0.84 (2.75)
Airfoil	NACA 65 ₁ -012
Rudder:	
Span, m (ft)	1.07 (3.50)
Area, m ² (ft ²)	0.34 (3.61)
Mean aerodynamic chord, m (ft)	0.29 (0.96)
Hinge line, percent of vertical-tail \bar{c}	65.5

TABLE I.- Concluded

Horizontal tail:

Span, m (ft)	2.34 (7.69)
Area, m ² (ft ²)	1.55 (16.74)
Incidence, deg	0.0
Root chord, m (ft)	1.10 (3.60)
Tip chord, m (ft)	0.51 (1.67)
Mean aerodynamic chord, m (ft)	0.84 (2.75)
Airfoil section	NACA 65 ₁ -012

Elevator:

Span, m (ft)	2.34 (7.69)
Area, m ² (ft ²)	0.67 (7.22)
Mean aerodynamic chord, m (ft)	0.29 (0.96)
Hinge line, percent \bar{c}_t	65.5

Tail spoiler:

Span, m (ft)	2.09 (6.86)
Area, m ² (ft ²)	0.11 (1.14)
Constant chord, m (ft)	0.05 (0.17)
Hinge line, percent \bar{c}_t	59.4

Propeller:

Diameter, m (ft)	1.80 (5.92)
------------------------	-------------

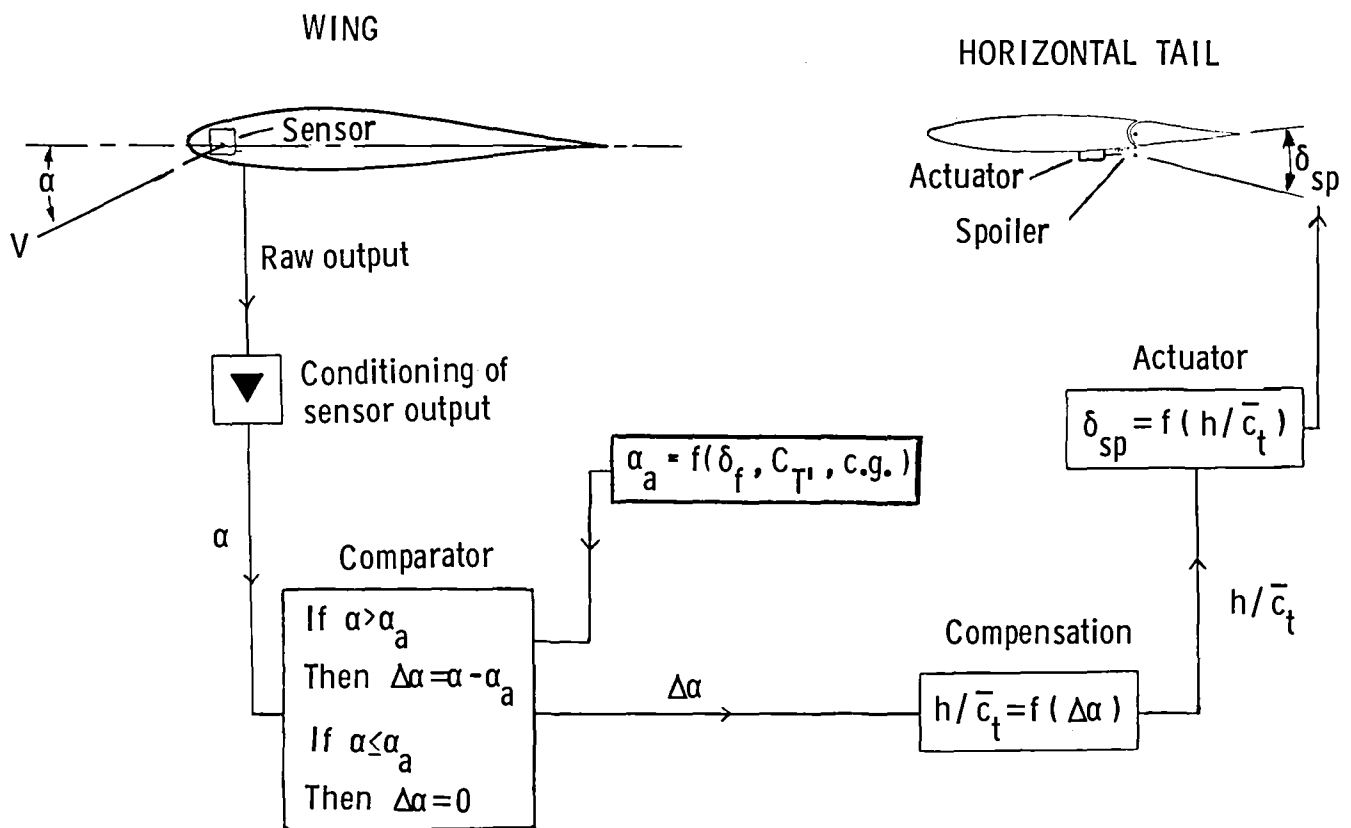


Figure 1.- Tail-spoiler stall-prevention system.

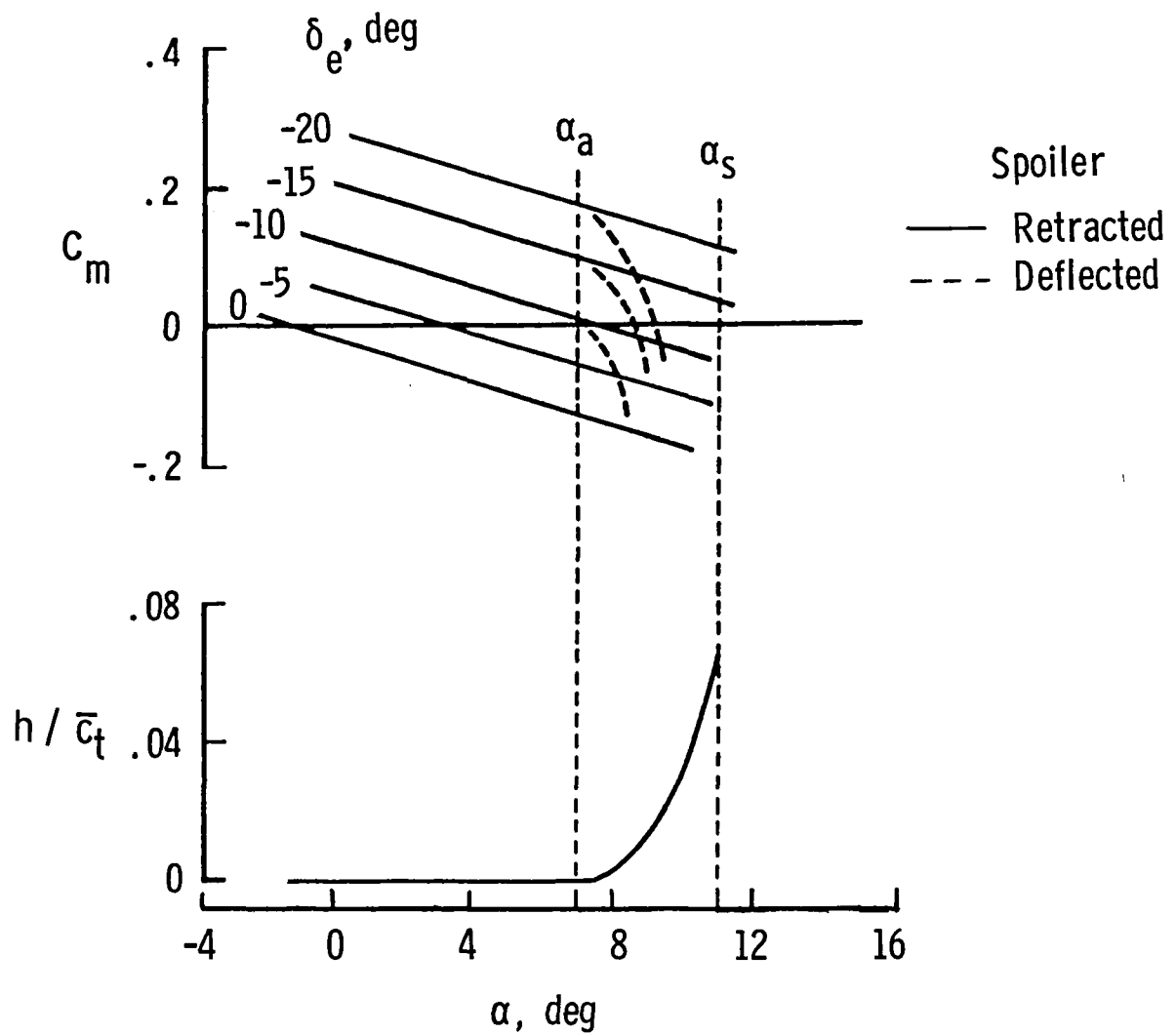


Figure 2.- Predicted tail spoiler deployment and pitching-moment characteristics.

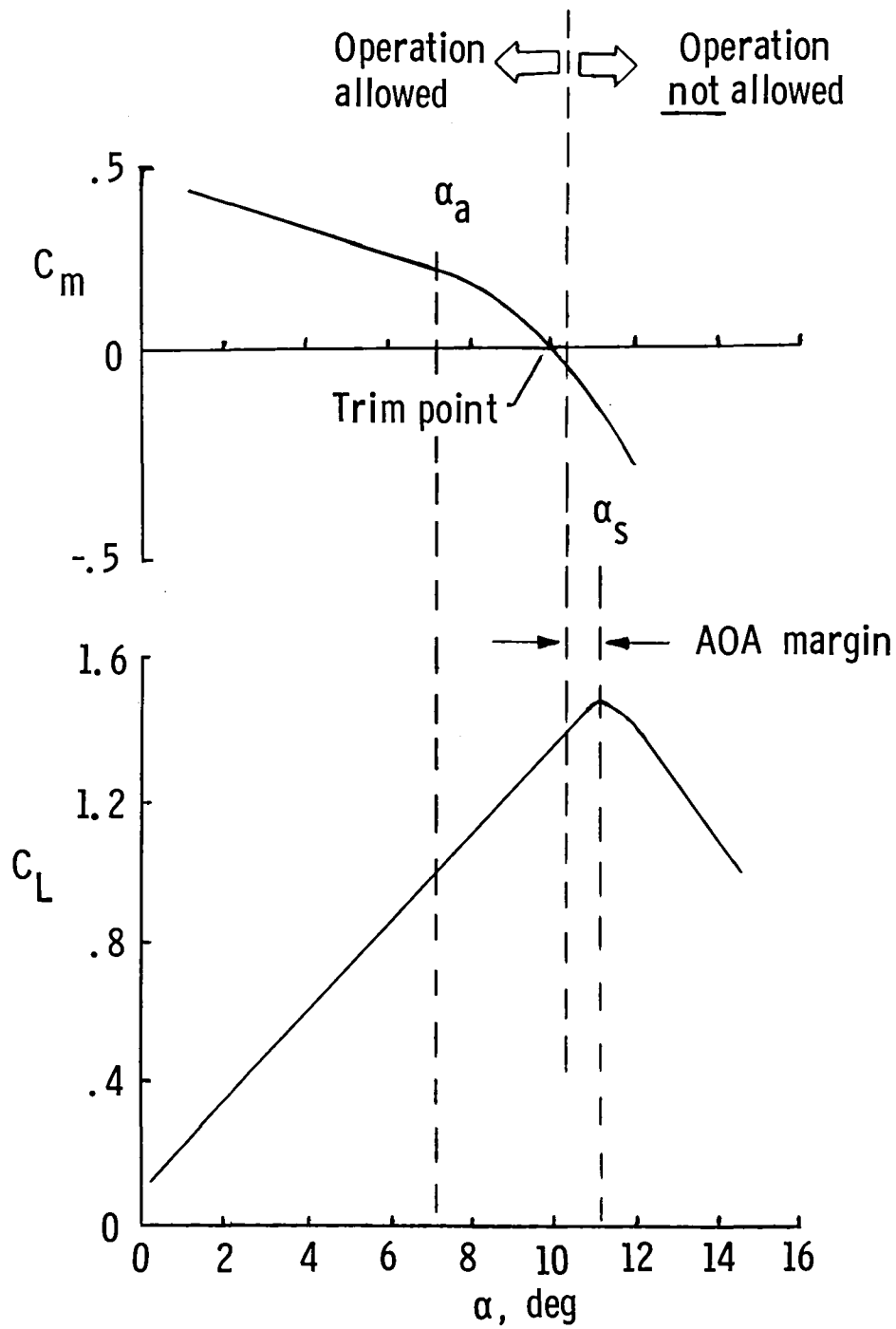


Figure 3.- Operating boundaries for a stall-prevention system.

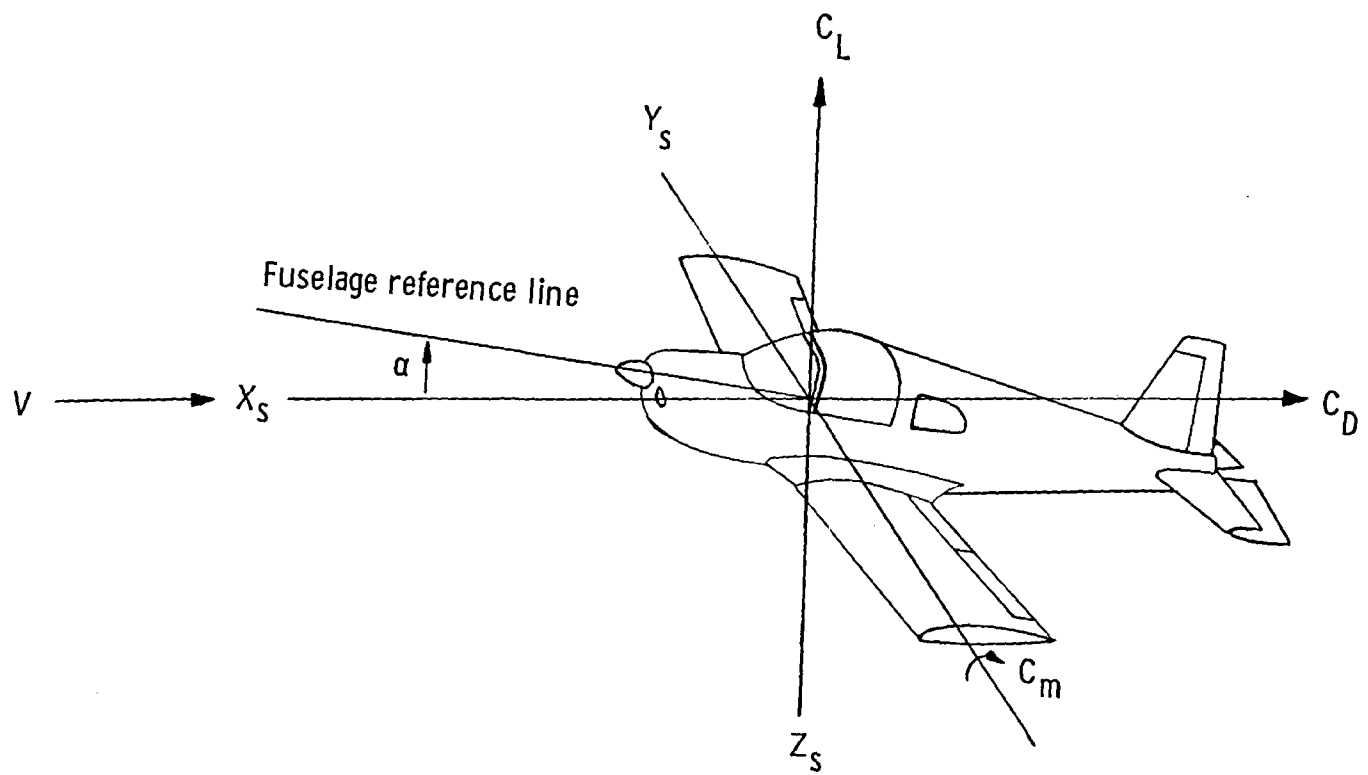


Figure 4.- Stability axes.

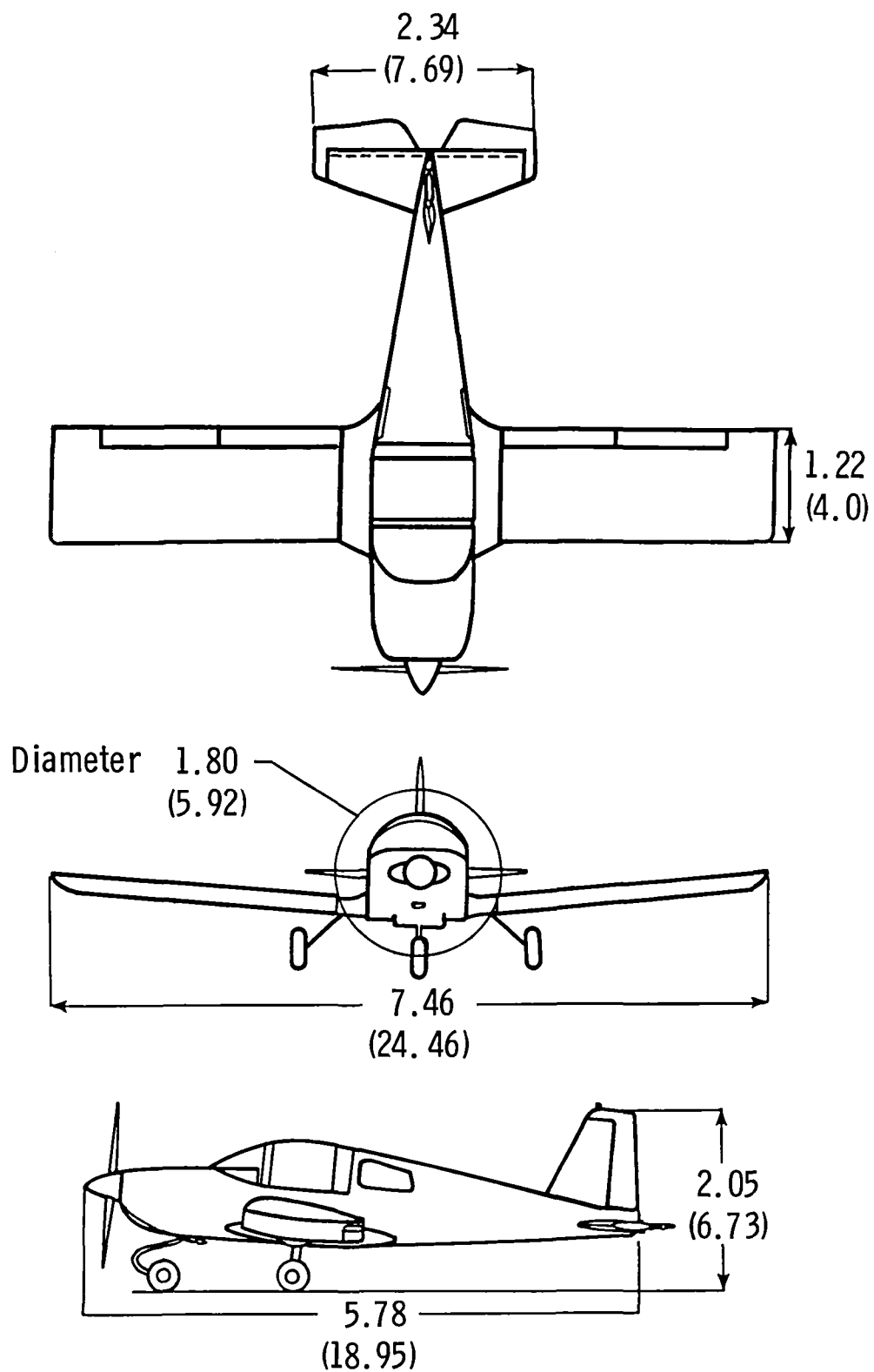
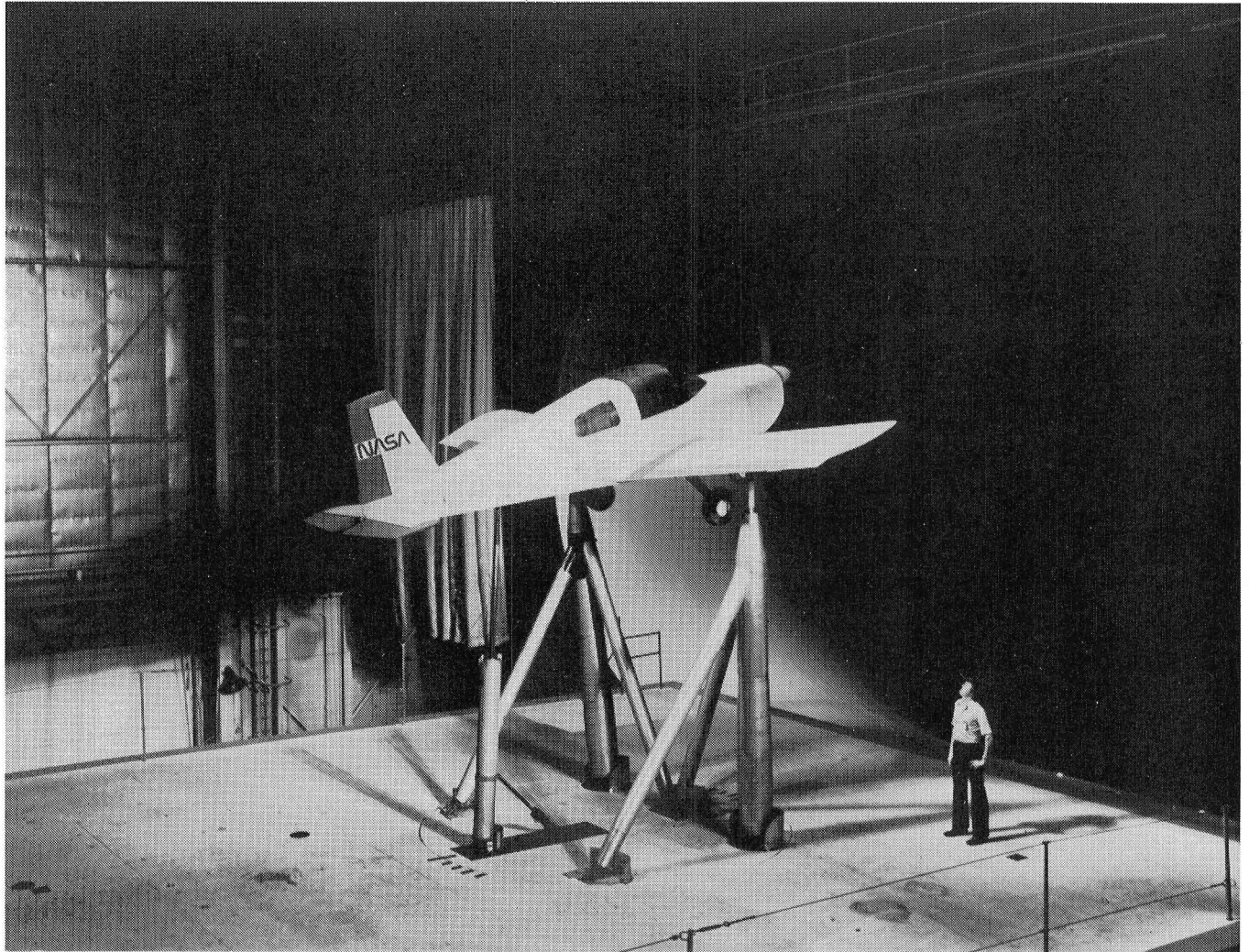
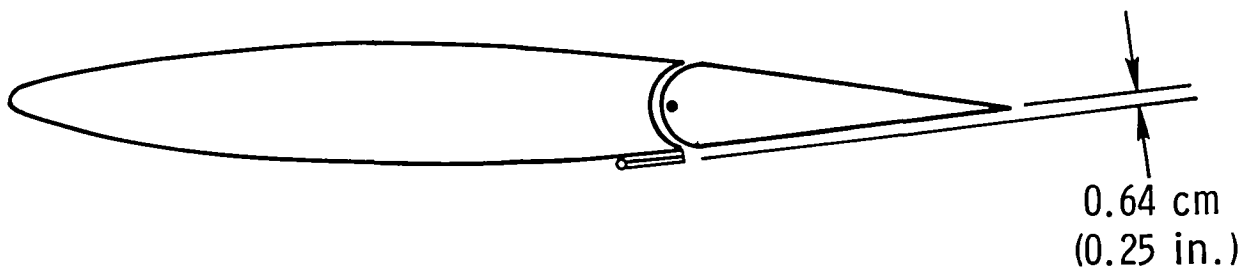


Figure 5.- Wind-tunnel model. Dimensions are in meters (feet).

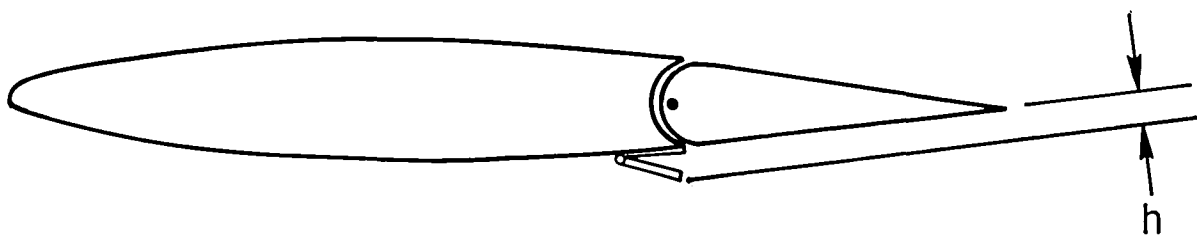


L-81-2299

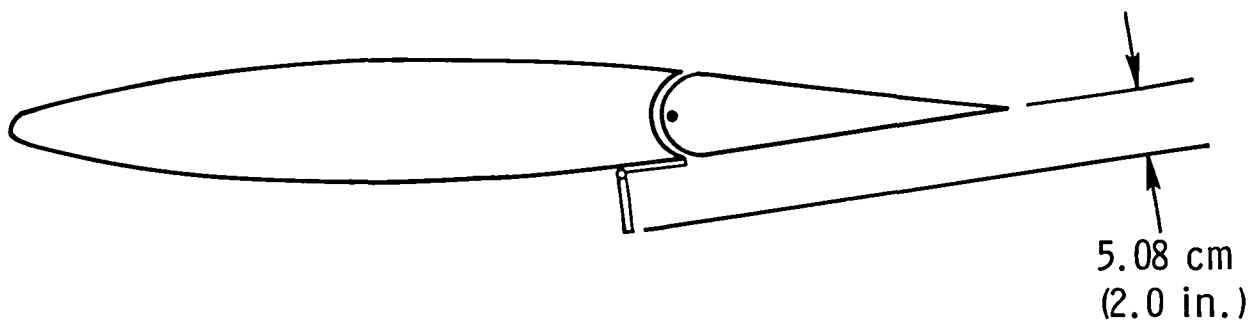
Figure 6.- Model installed in the Langley 30- by 60-Foot Wind Tunnel.



(a) Retracted, $h/\bar{c}_t = 0.007$ and $\delta_{sp} = 0^\circ$.



(b) Partially deflected.



(c) Fully deflected, $h/\bar{c}_t = 0.0605$ and $\delta_{sp} = 90^\circ$.

Figure 7.- Tail spoiler installation and deployment characteristics.

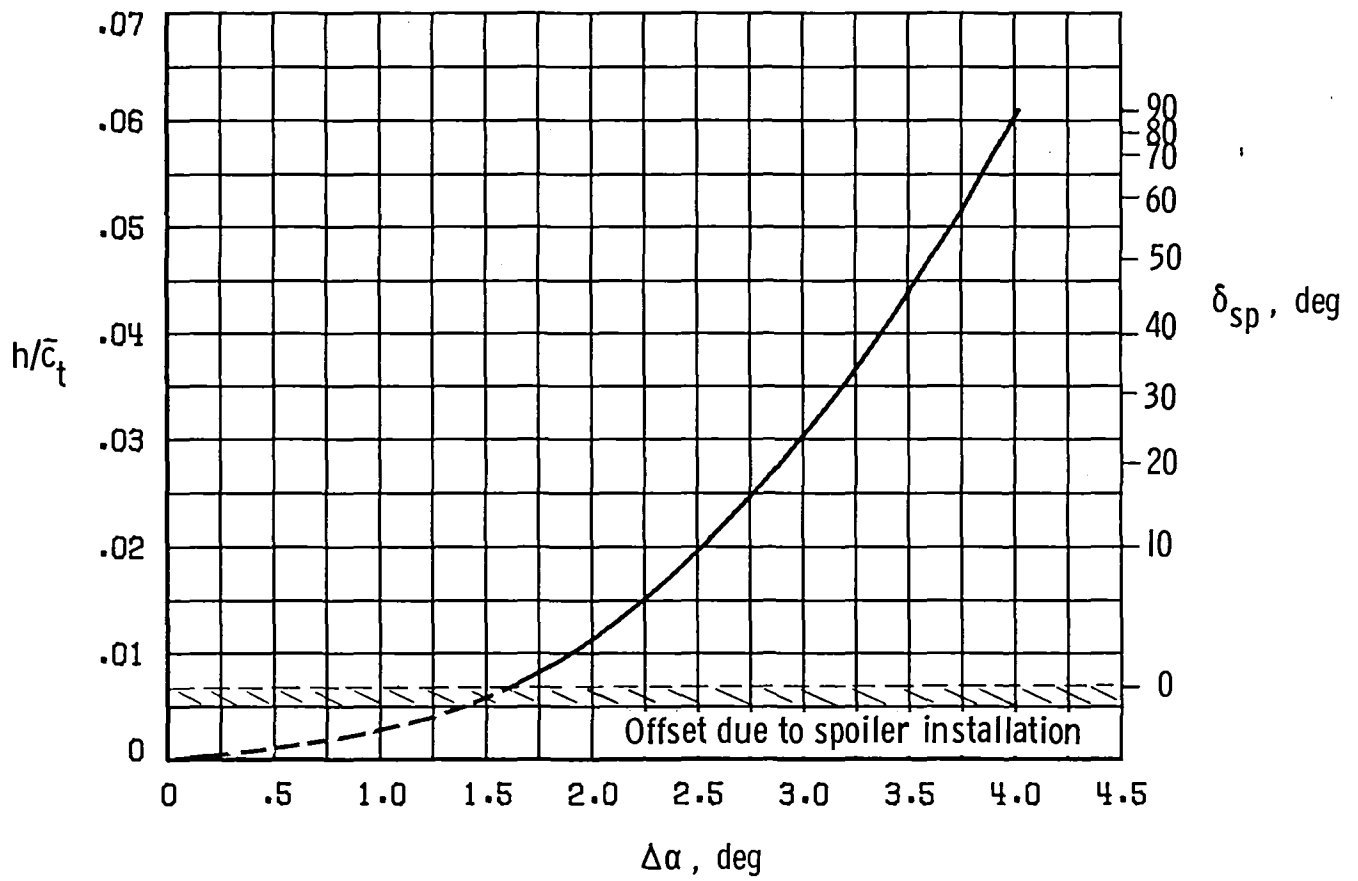


Figure 8.- Tail spoiler deployment schedule.



C_T	δ_f , deg
○	-0.01 0
□	.09 0
◇	.09 30
△	.25 30

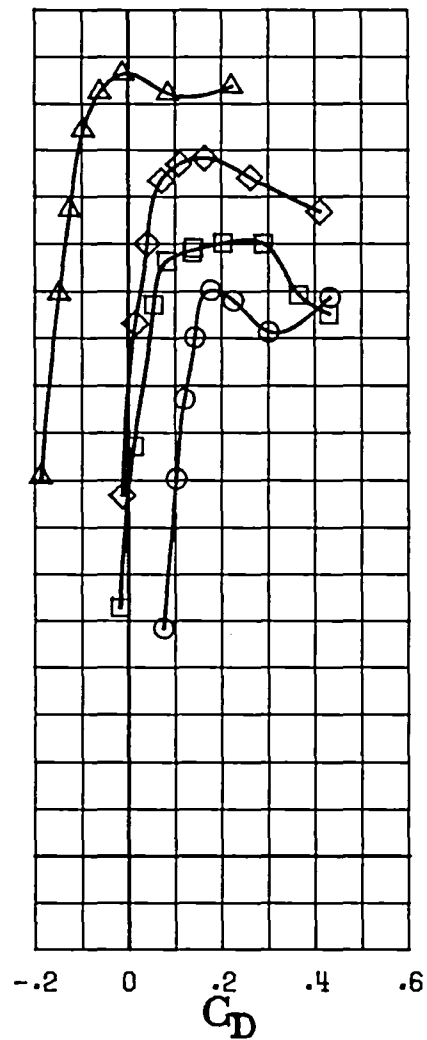
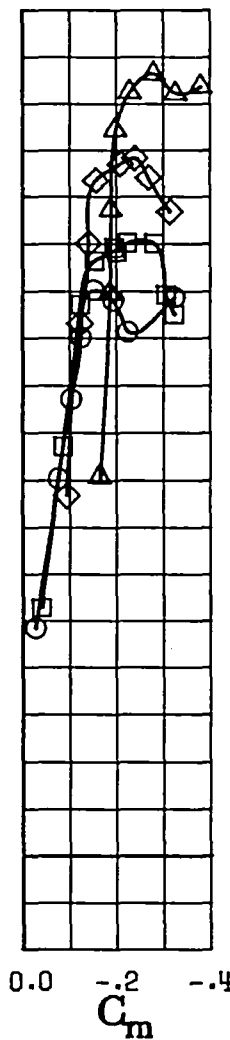
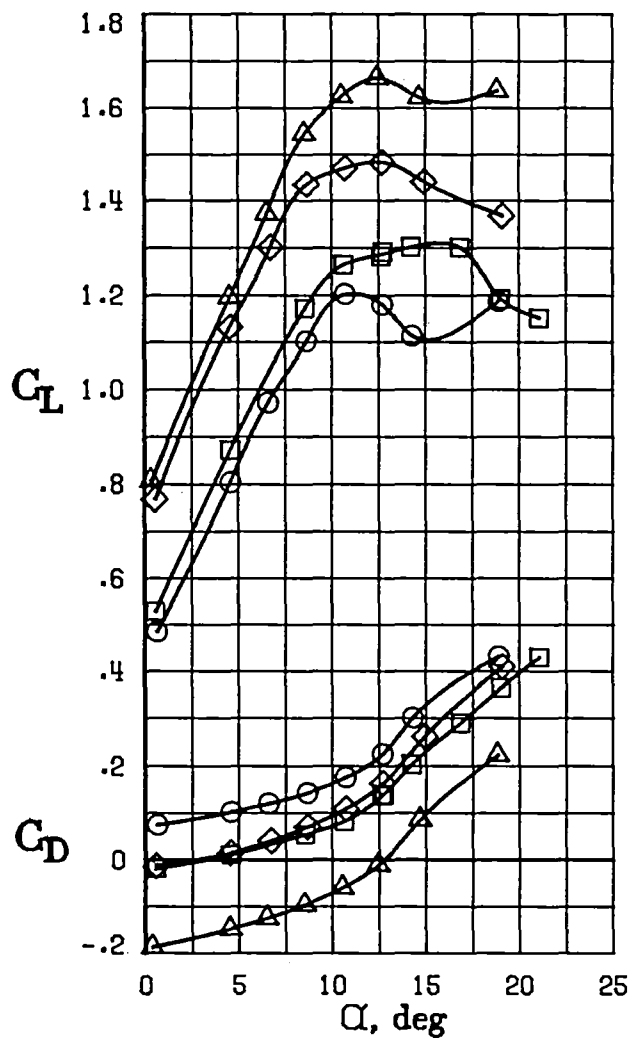
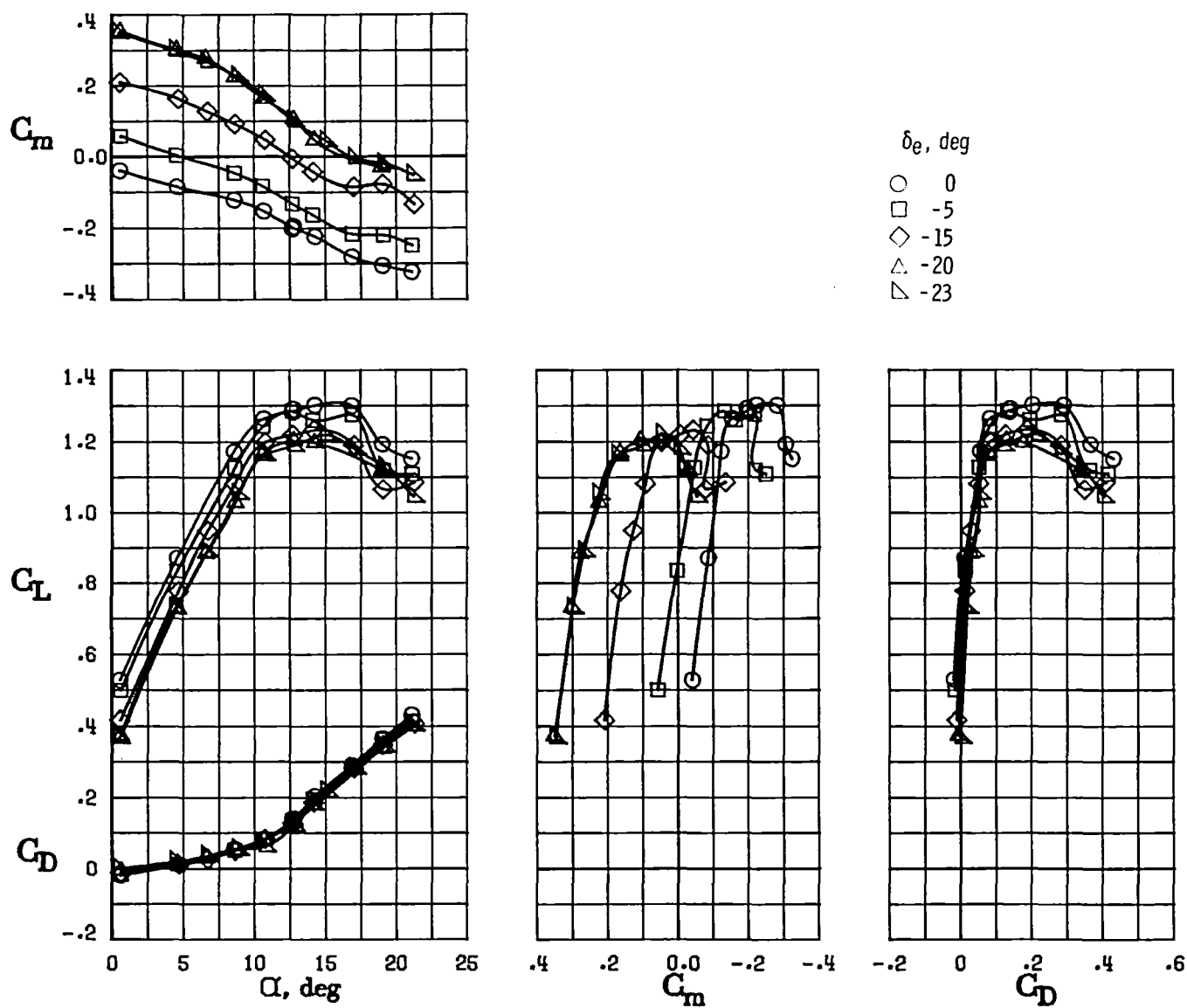
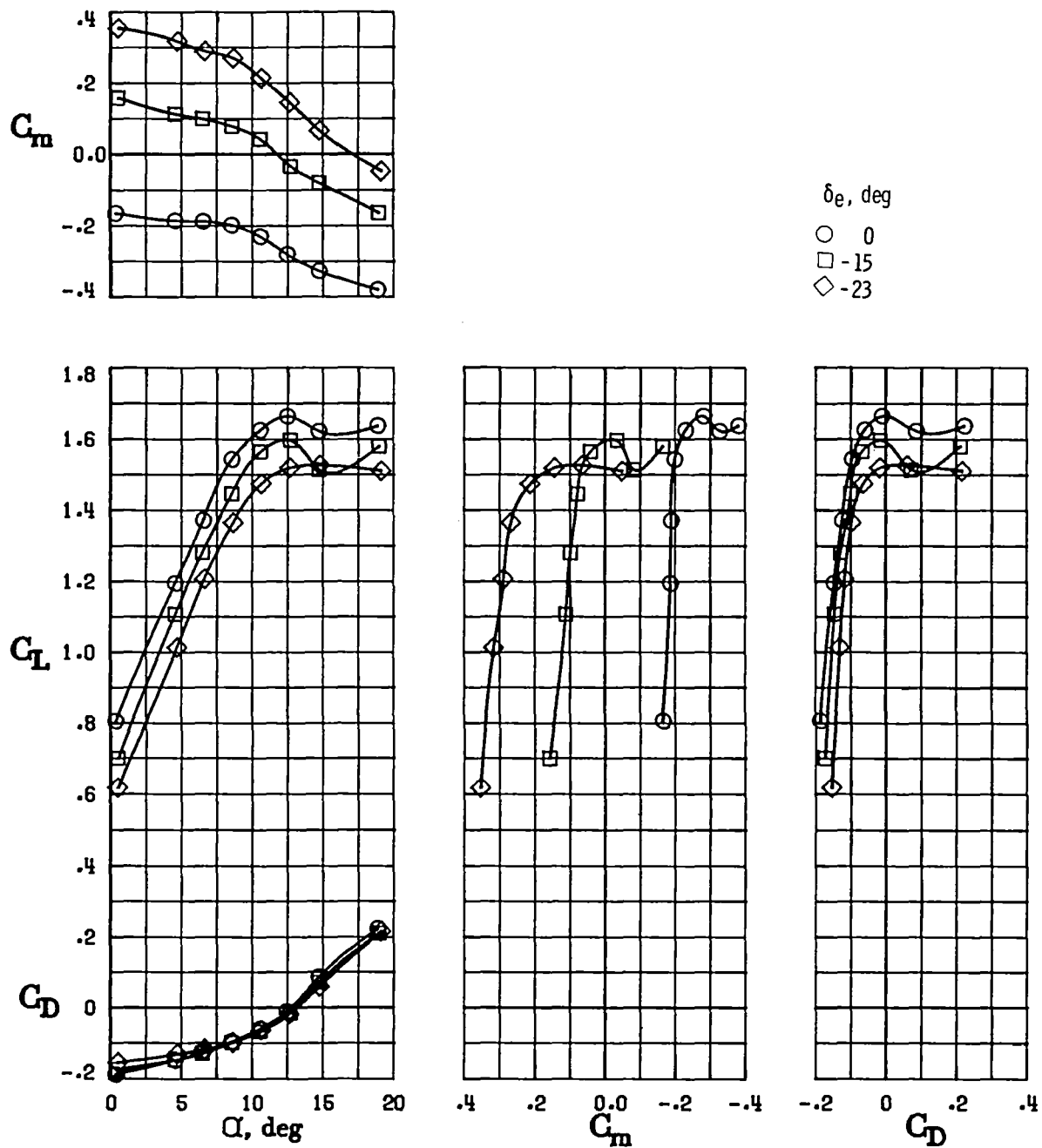


Figure 9.- Effect of power and flaps on longitudinal characteristics. $\delta_e = 0^\circ$.



(a) Cruise condition. $C_{T_1} = 0.09$; $\delta_f = 0^\circ$.

Figure 10.- Effect of elevator deflection on the longitudinal characteristics.



(b) Go-around condition. $C_{T1} = 0.25$; $\delta_f = 30^\circ$.

Figure 10.- Concluded.

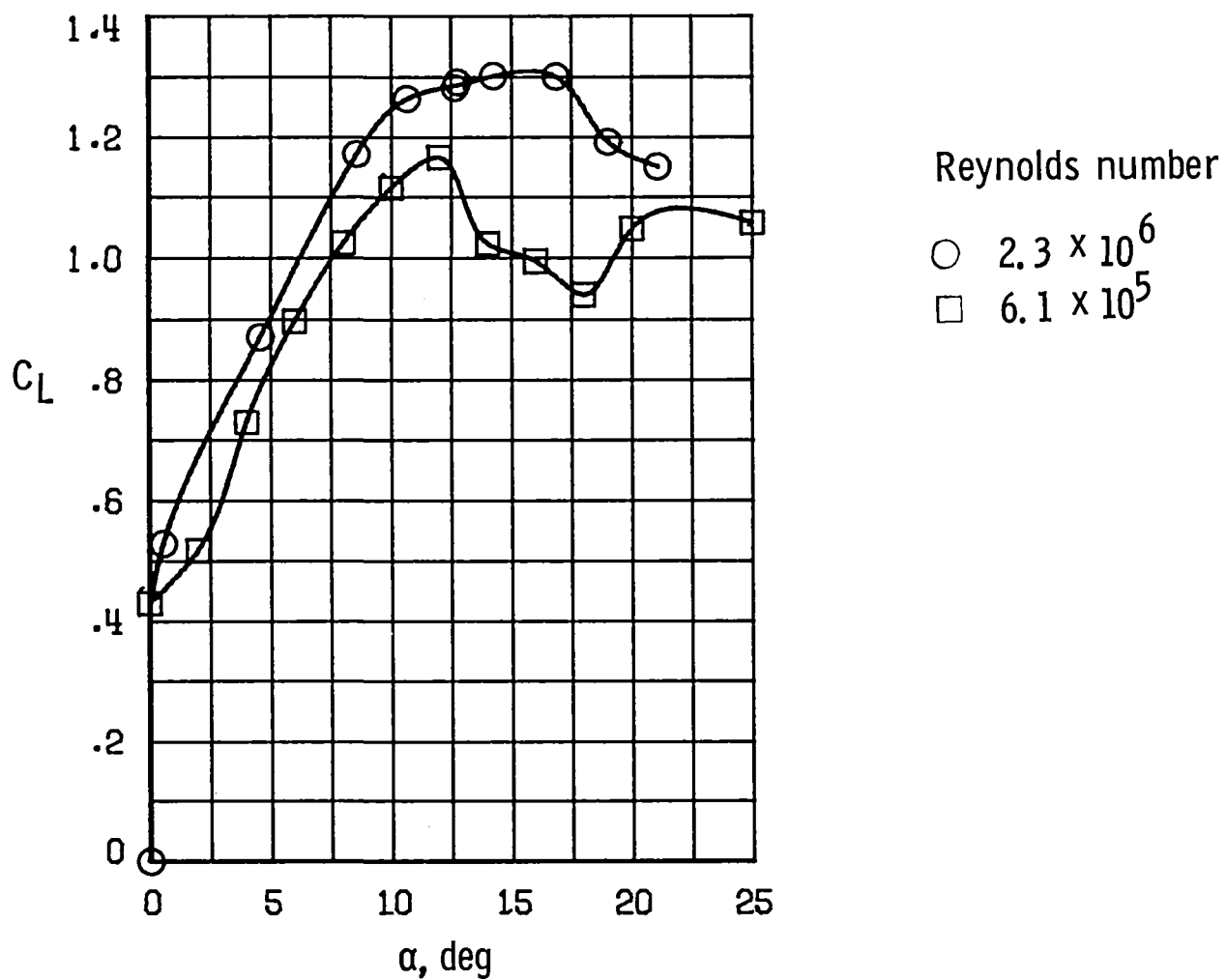
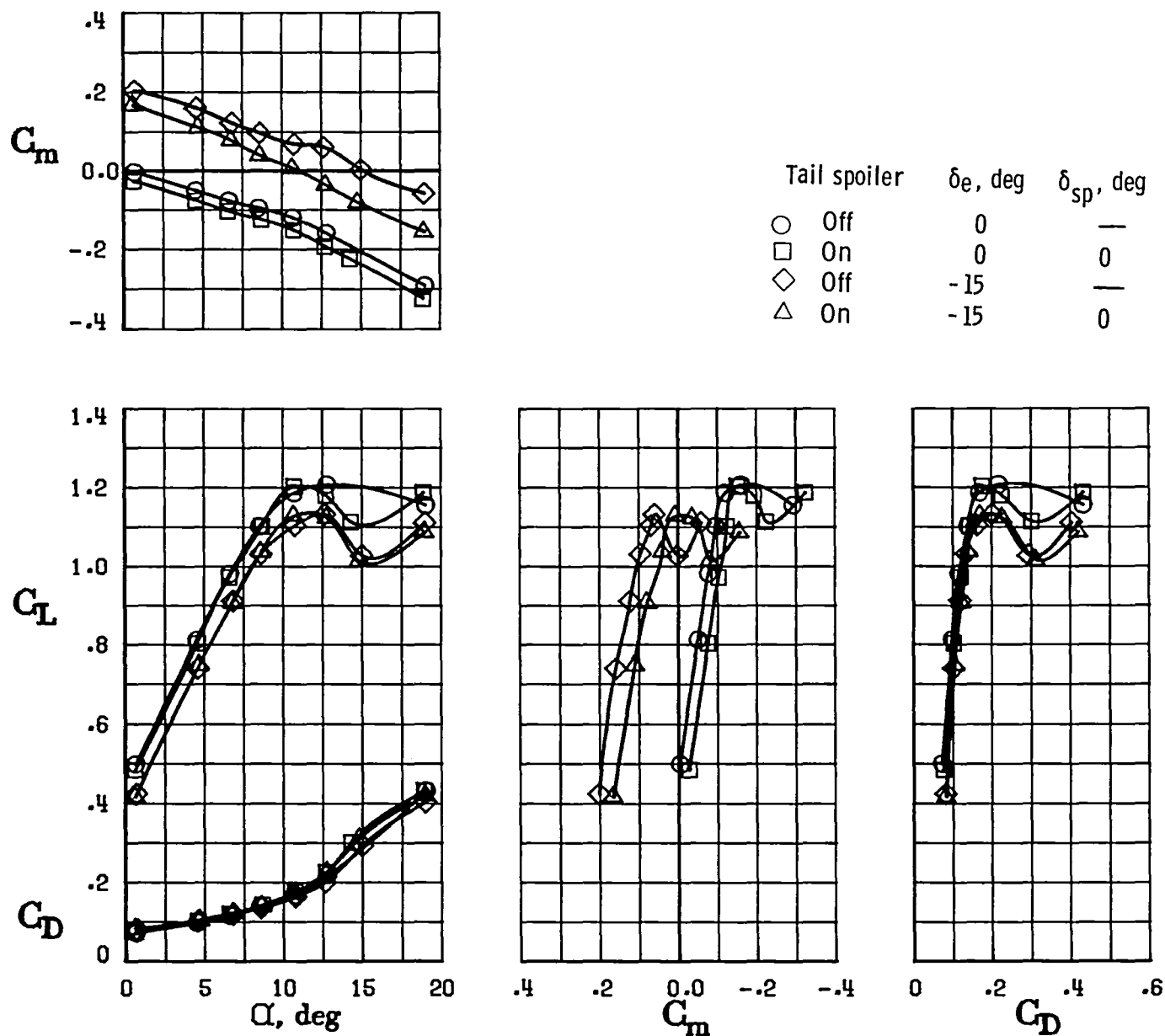
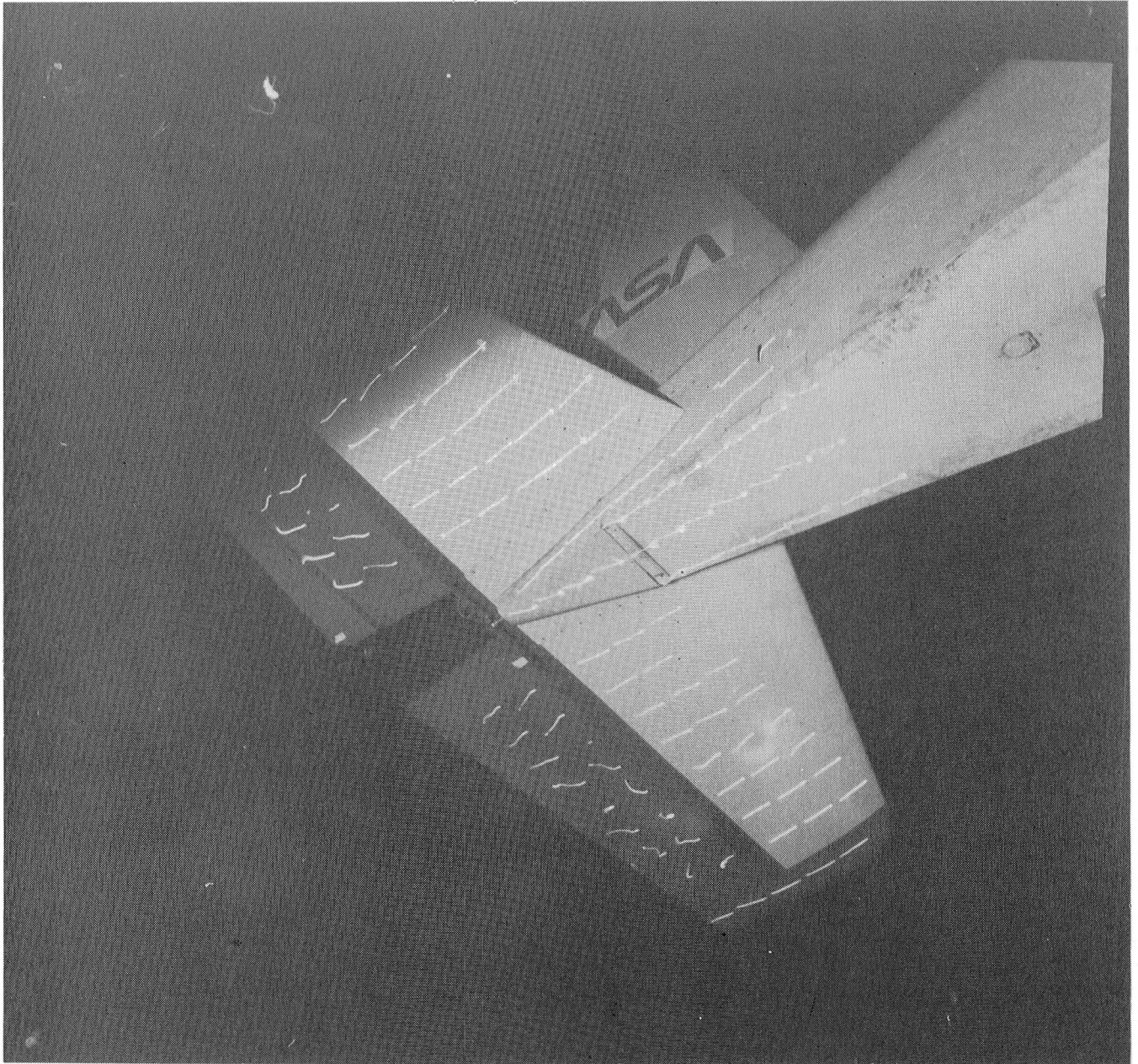


Figure 11.- Effect of Reynolds number on the longitudinal characteristics.
Cruise condition. $C_{T1} = 0.09$; $\delta_f = 0^\circ$; $\delta_e = 0^\circ$.



(a) Longitudinal characteristics.

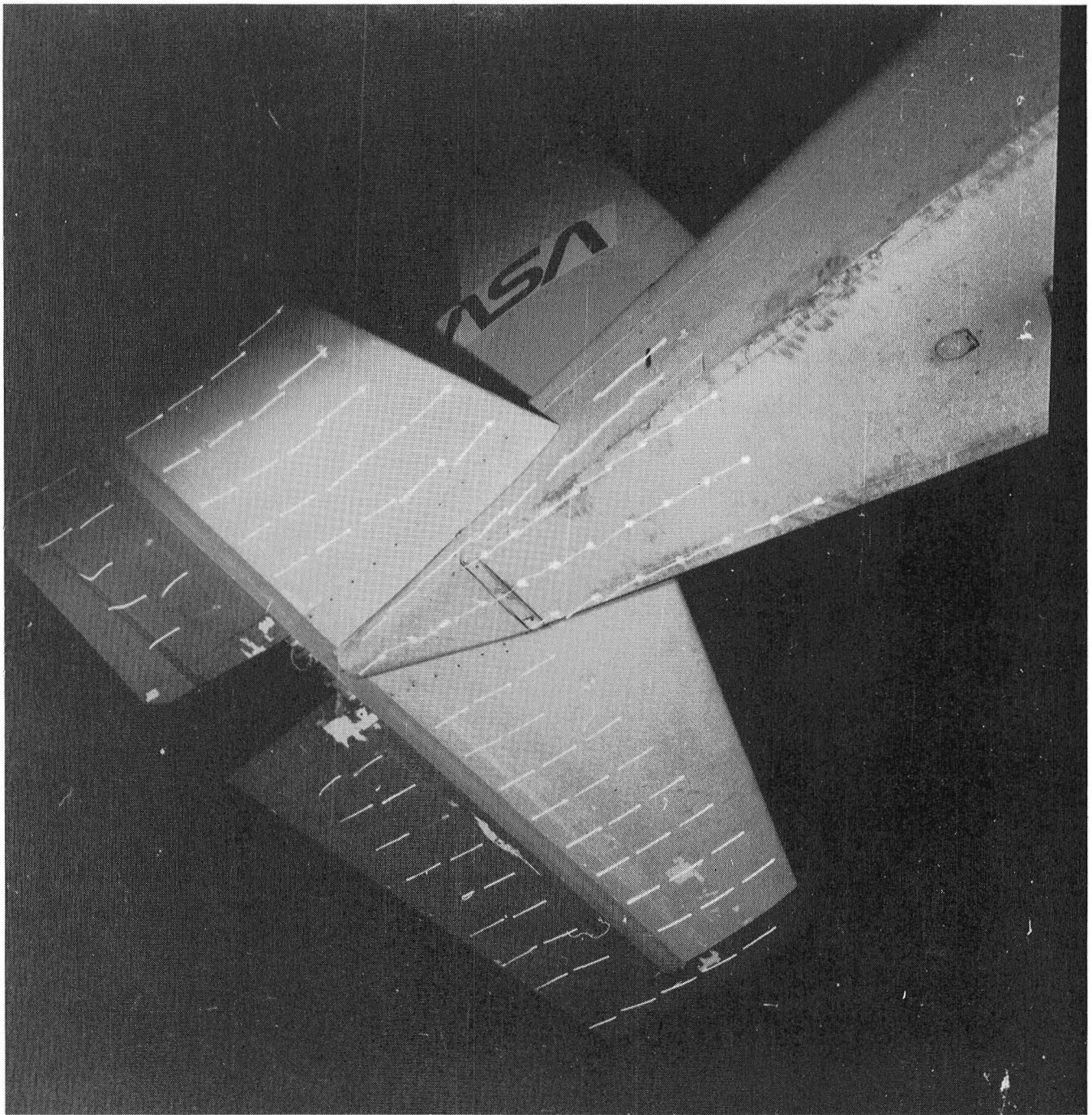
Figure 12.- Effect of the tail-spoiler installation on the model. Power-off condition. $C_{T_1} = -0.01$; $\delta_f = 0^\circ$.



L-81-225

(b) Tuft characteristics without tail spoiler.

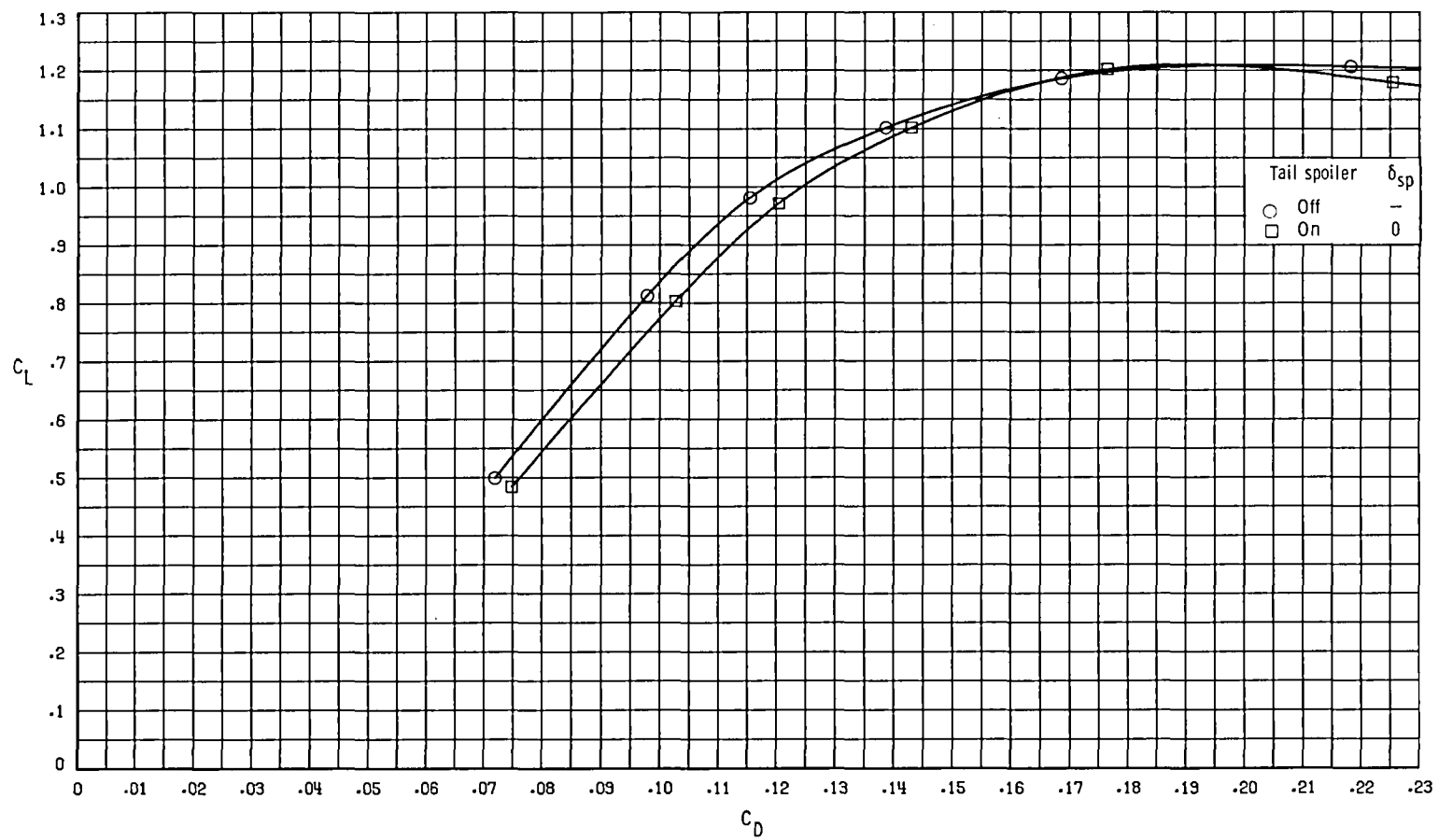
Figure 12.- Continued.



L-81-226

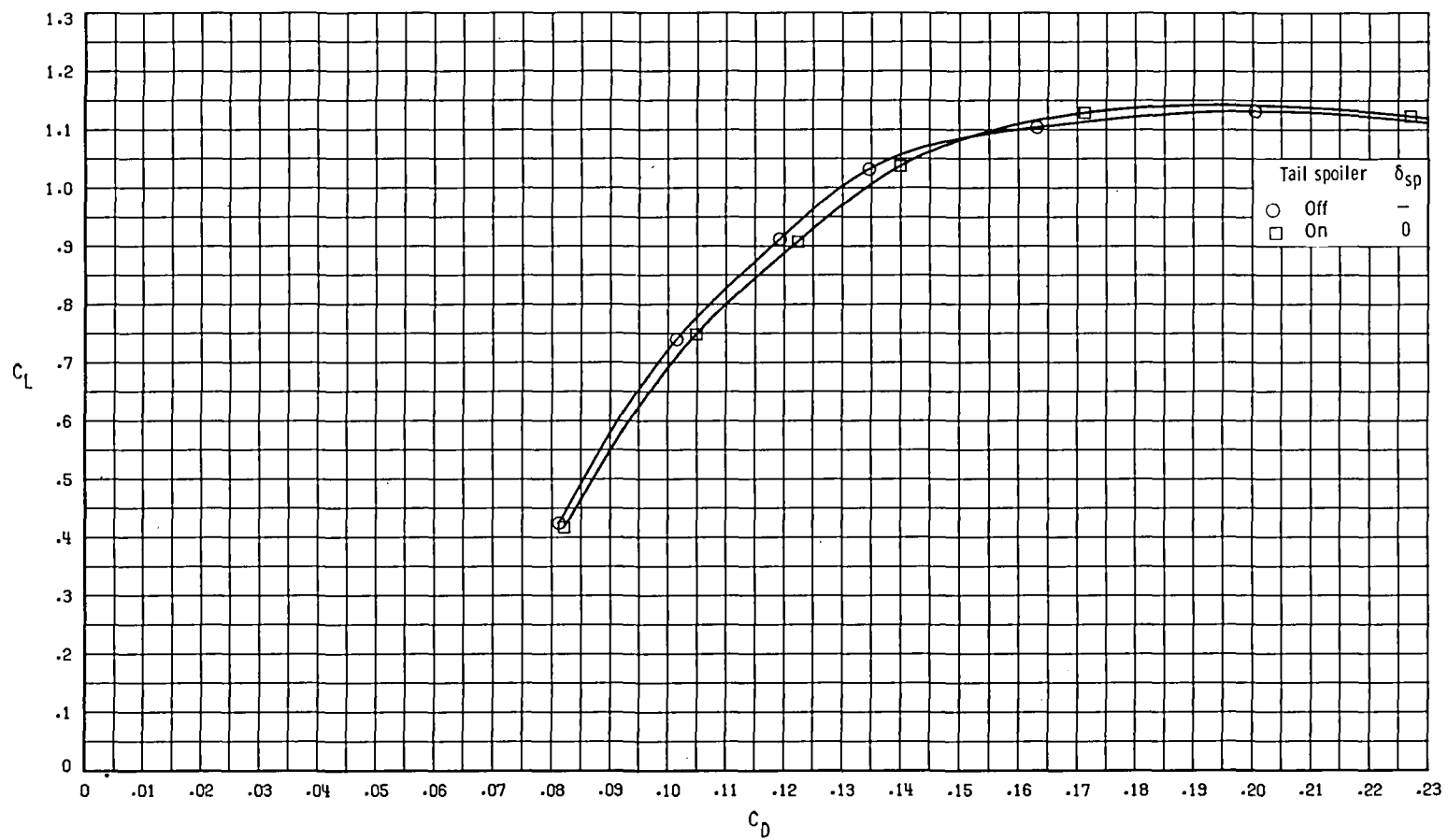
(c) Tuft characteristics with tail spoiler installed. $\delta_{sp} = 0^\circ$.

Figure 12.- Continued.



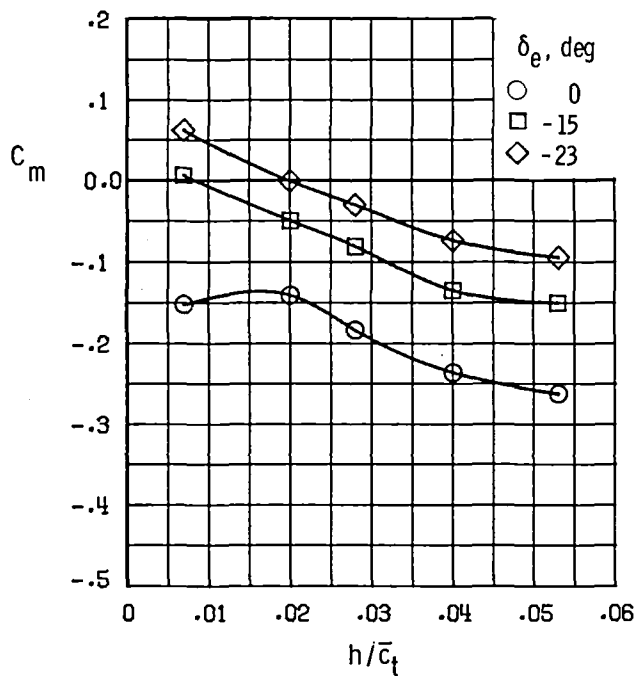
(d) Expanded lift-drag polar. $\delta_e = 0^\circ$.

Figure 12.- Continued.

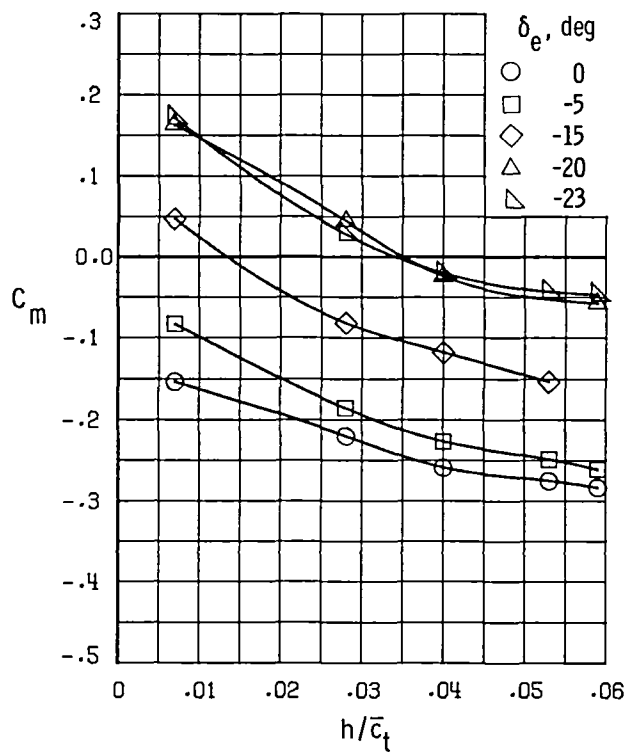


(e) Expanded lift-drag polar. $\delta_e = -15^\circ$.

Figure 12.- Concluded.

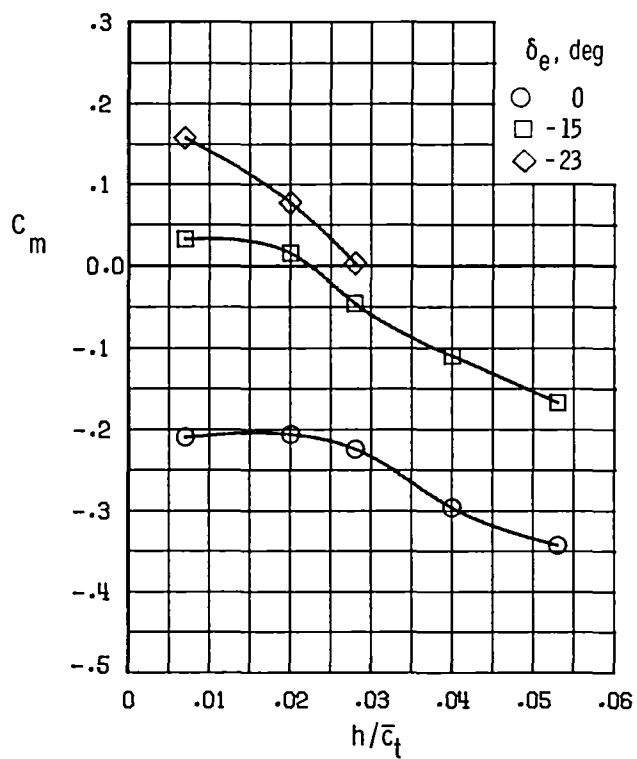


(a) Power-off condition. $C_{T,} = -0.01$;
 $\delta_f = 0^\circ$.

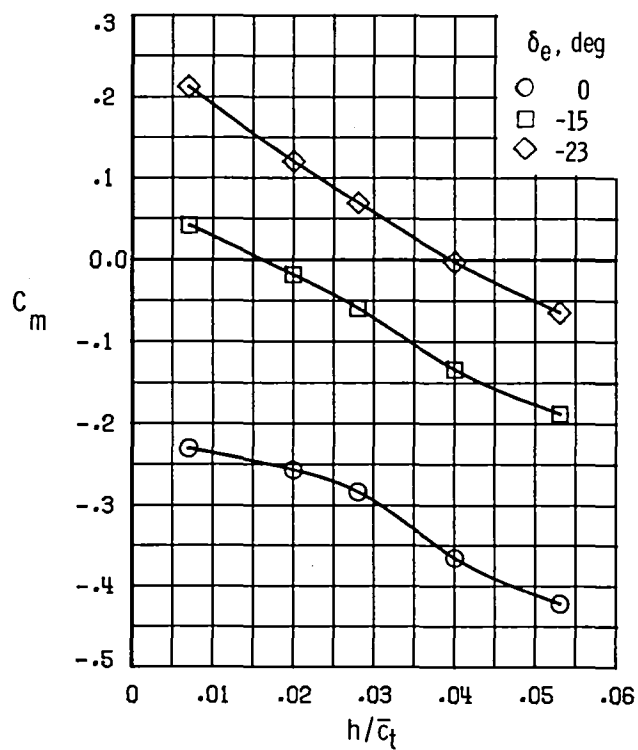


(b) Cruise condition. $C_{T,} = 0.09$;
 $\delta_f = 0^\circ$.

Figure 13.- Variation of the pitching-moment coefficient with tail-spoiler deflection. $\alpha = 10.5^\circ$.



(c) Approach condition. $C_{T1} = 0.09$;
 $\delta_f = 30^\circ$.



(d) Go-around condition. $C_{T1} = 0.25$;
 $\delta_f = 30^\circ$.

Figure 13.- Concluded.

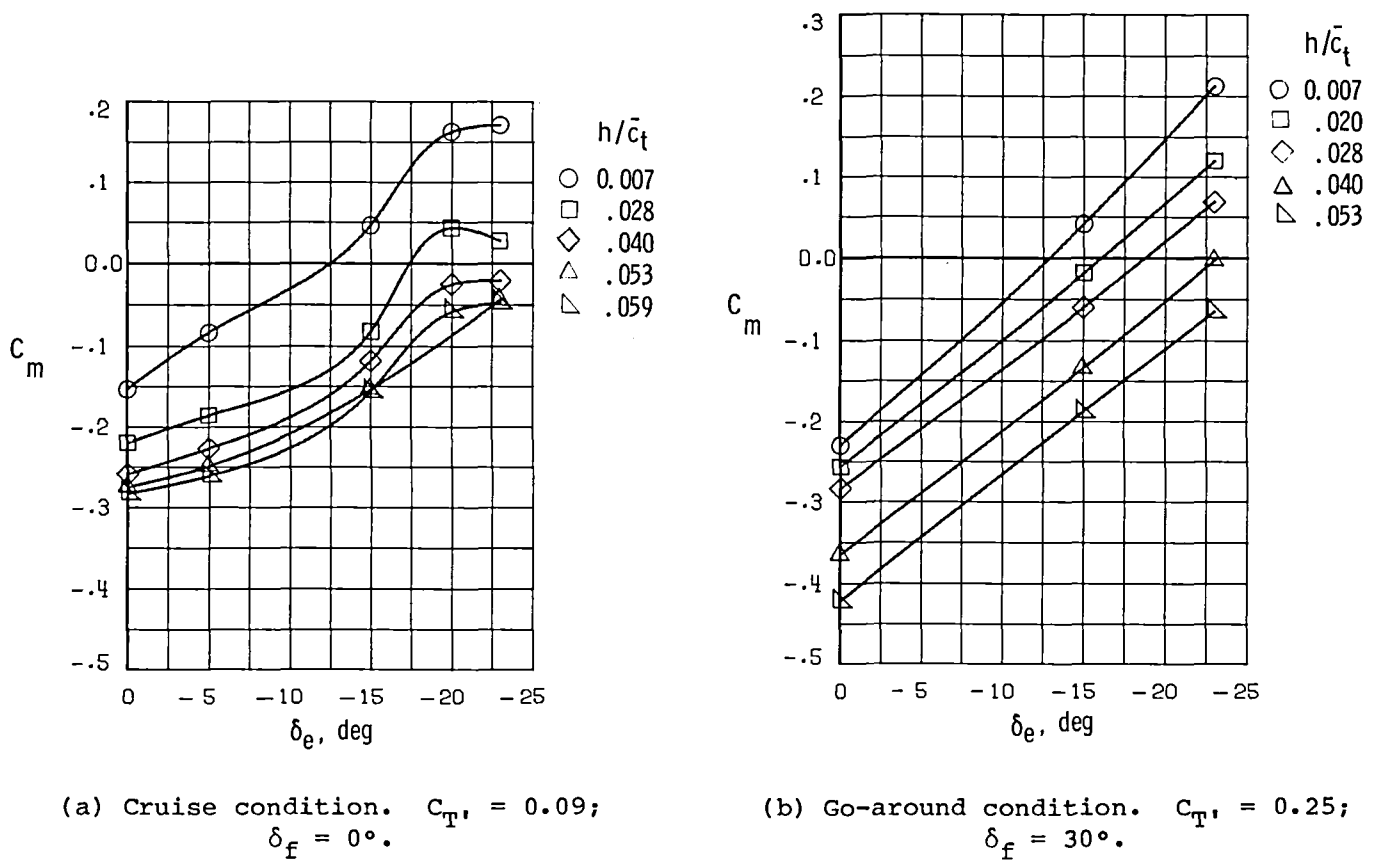


Figure 14.- Variation of the pitching-moment coefficient with elevator deflection for several tail-spoiler deflections. $\alpha = 10.5^\circ$.

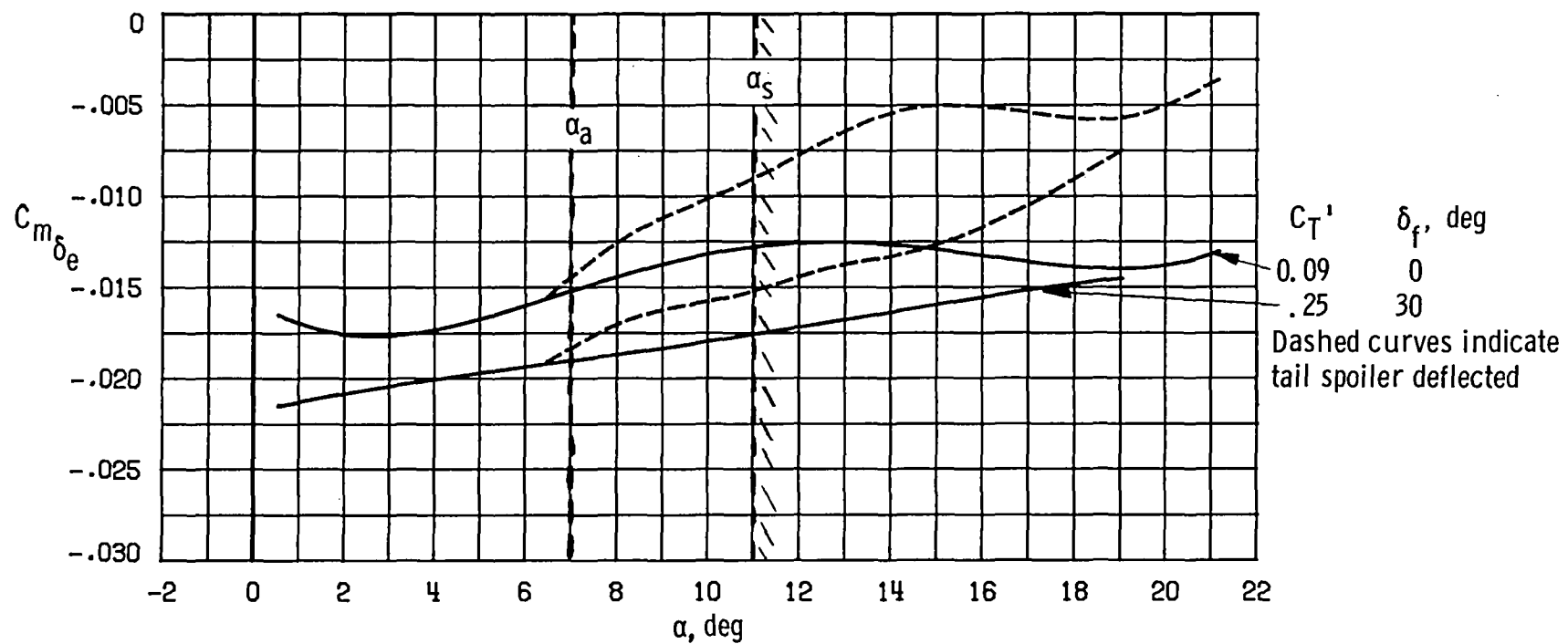
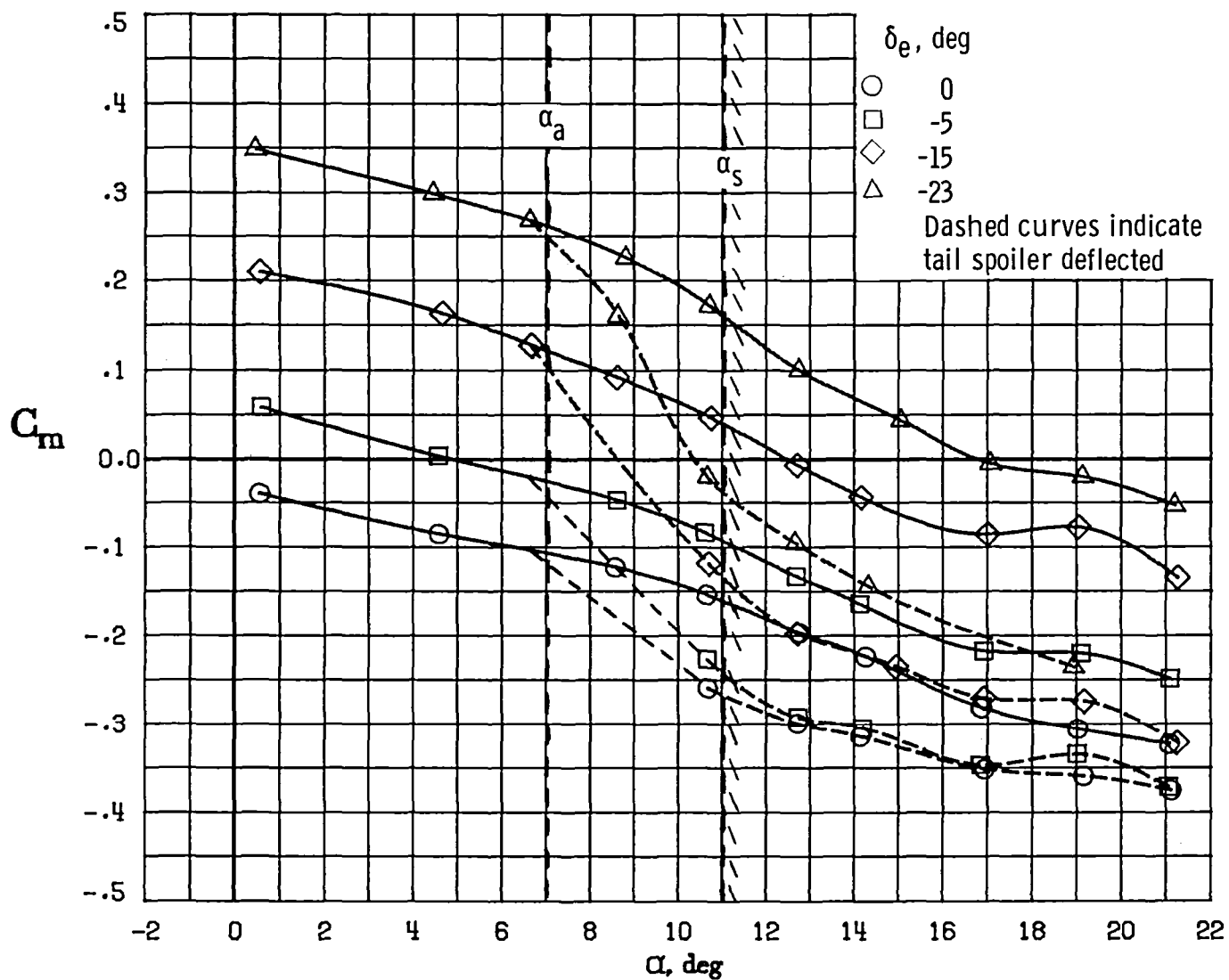
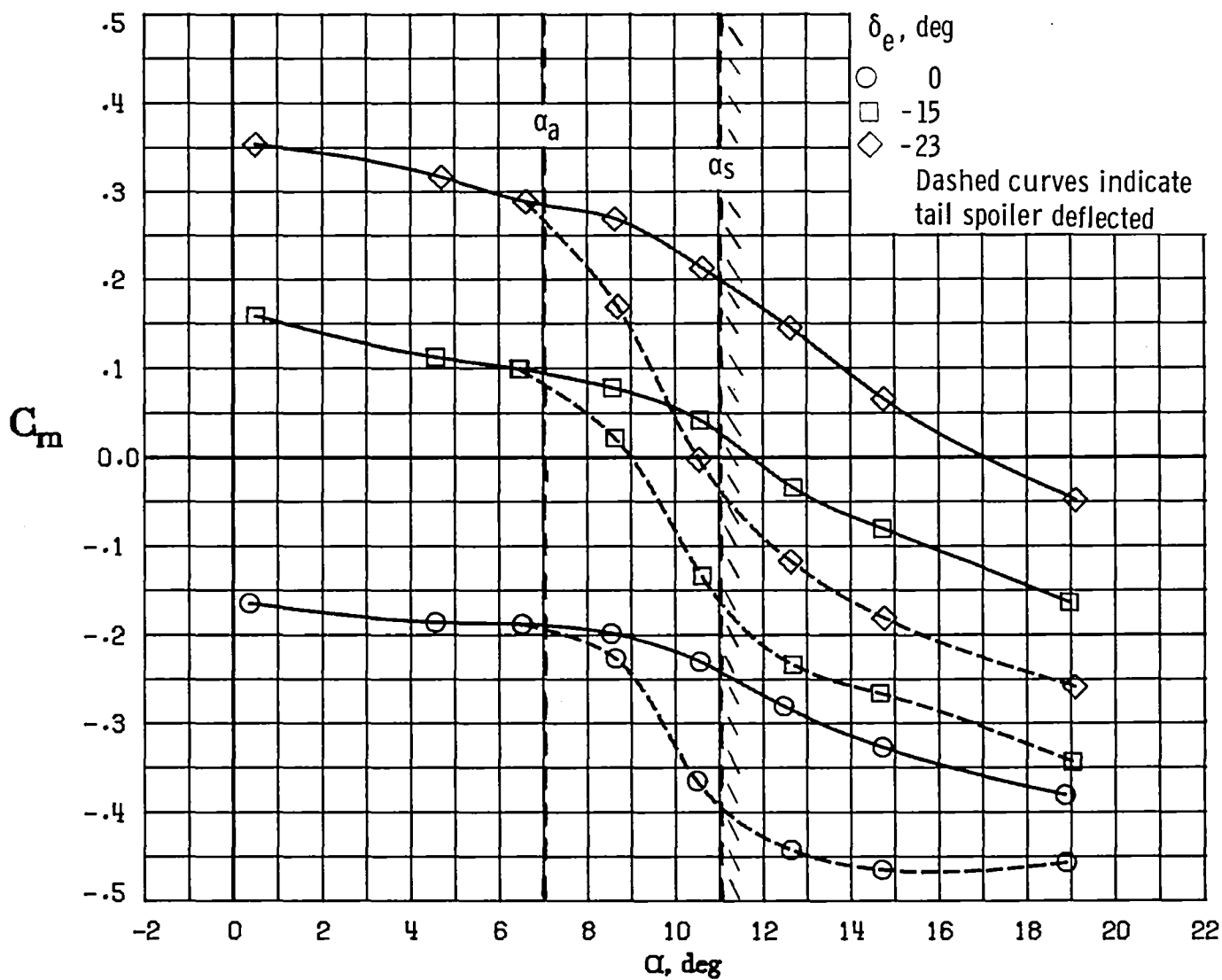


Figure 15.- Effect of tail-spoiler deflection on elevator effectiveness with power and flap effects.



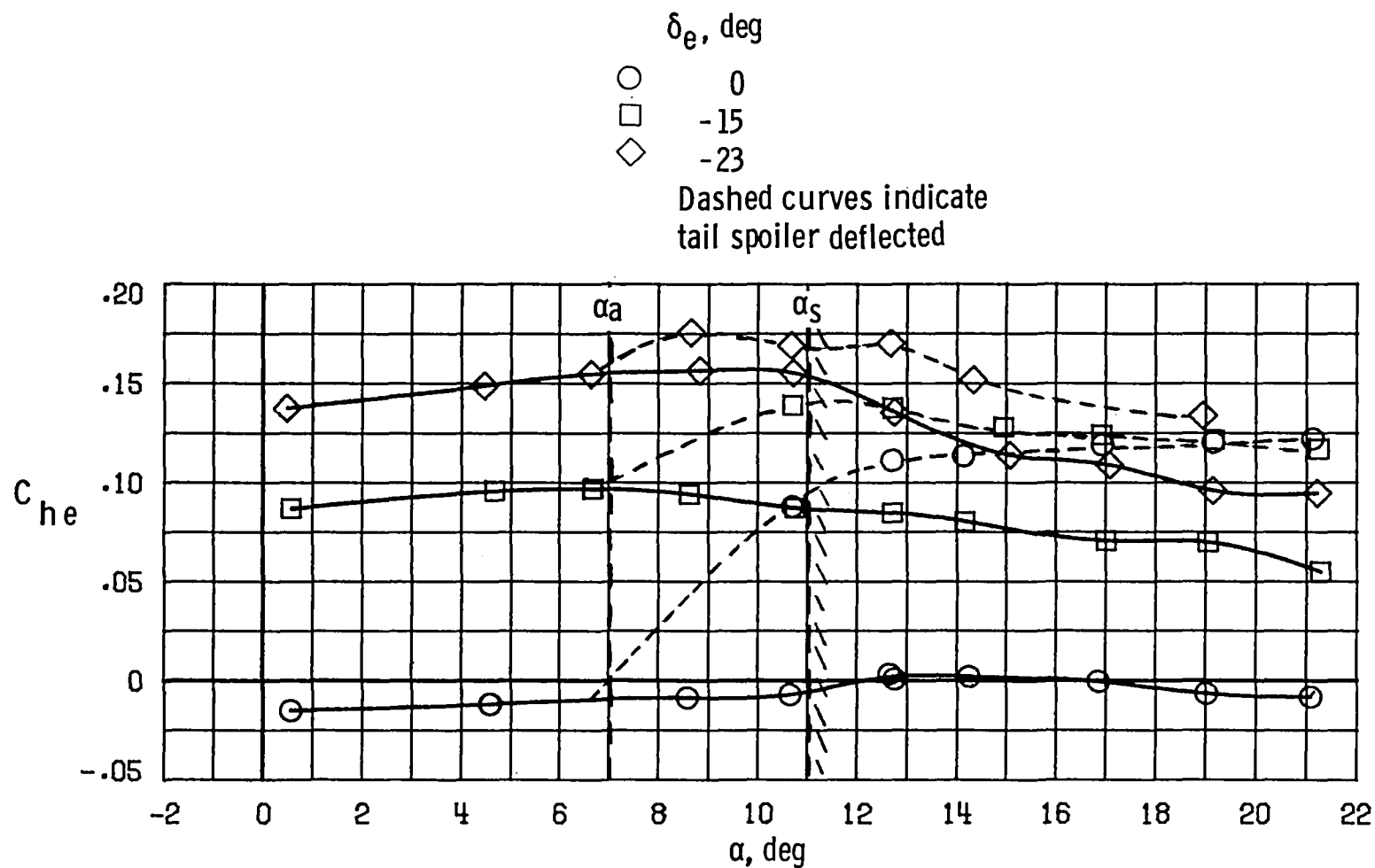
(a) Cruise condition. $C_{T_1} = 0.09$; $\delta_f = 0^\circ$.

Figure 16.- Effect of tail-spoiler deflection on variation of the pitching-moment coefficient with angle of attack.



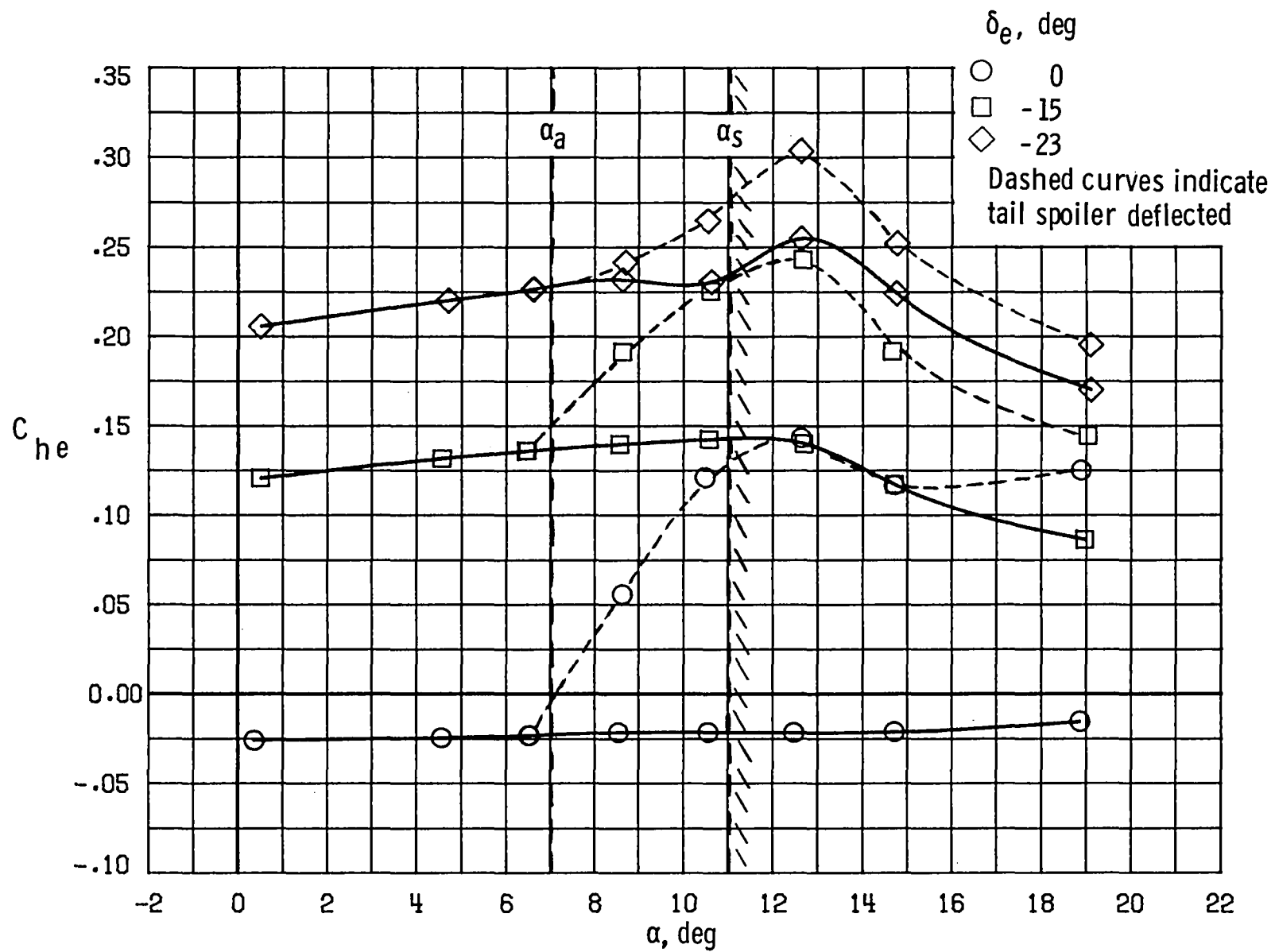
(b) Go-around condition. $C_{T1} = 0.25$; $\delta_f = 30^\circ$.

Figure 16.- Concluded.



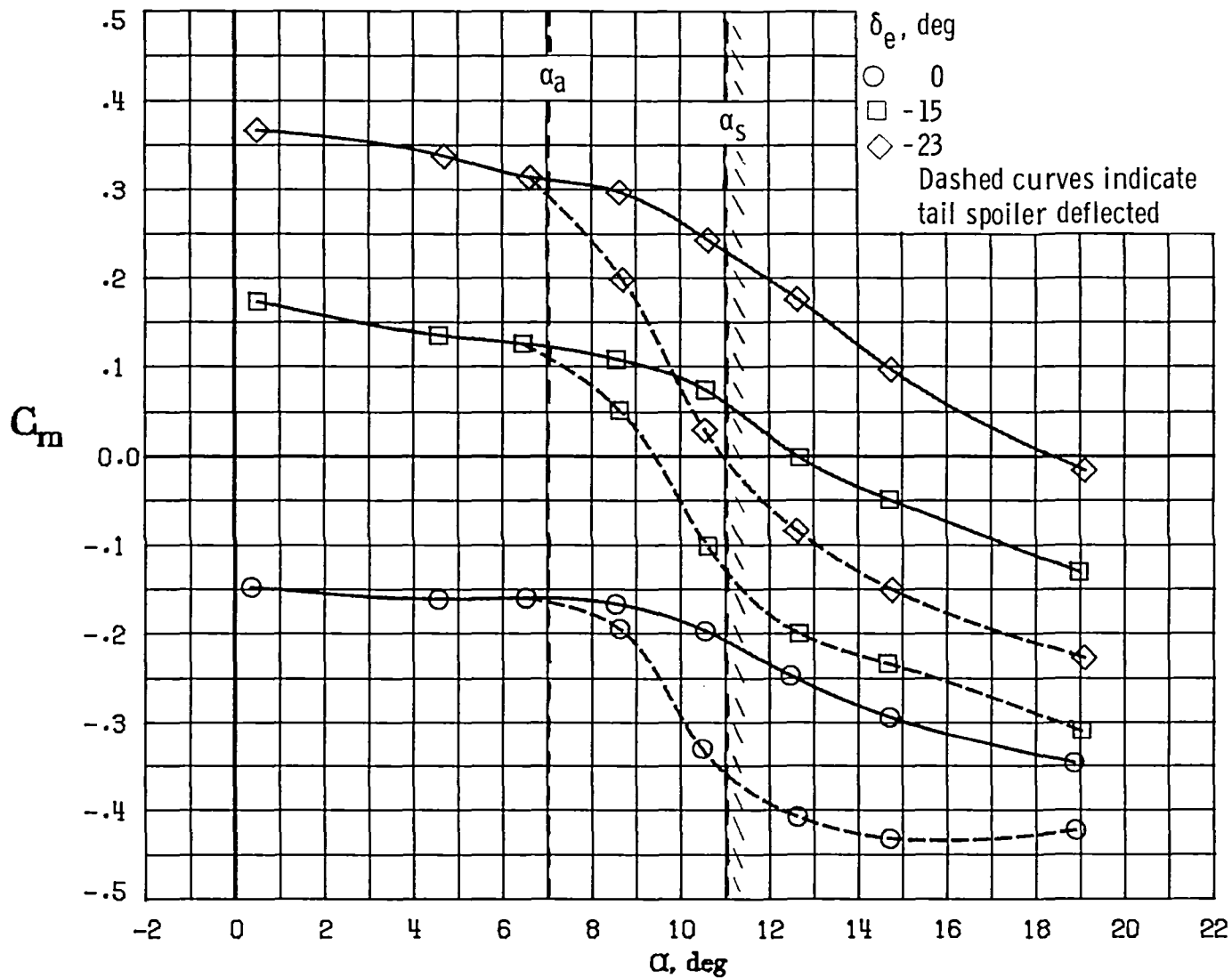
(a) Cruise condition. $C_{T1} = 0.09$ and $\delta_f = 0^\circ$.

Figure 17.- Effect of tail-spoiler deflection on variation of elevator hinge moment coefficient with angle of attack.



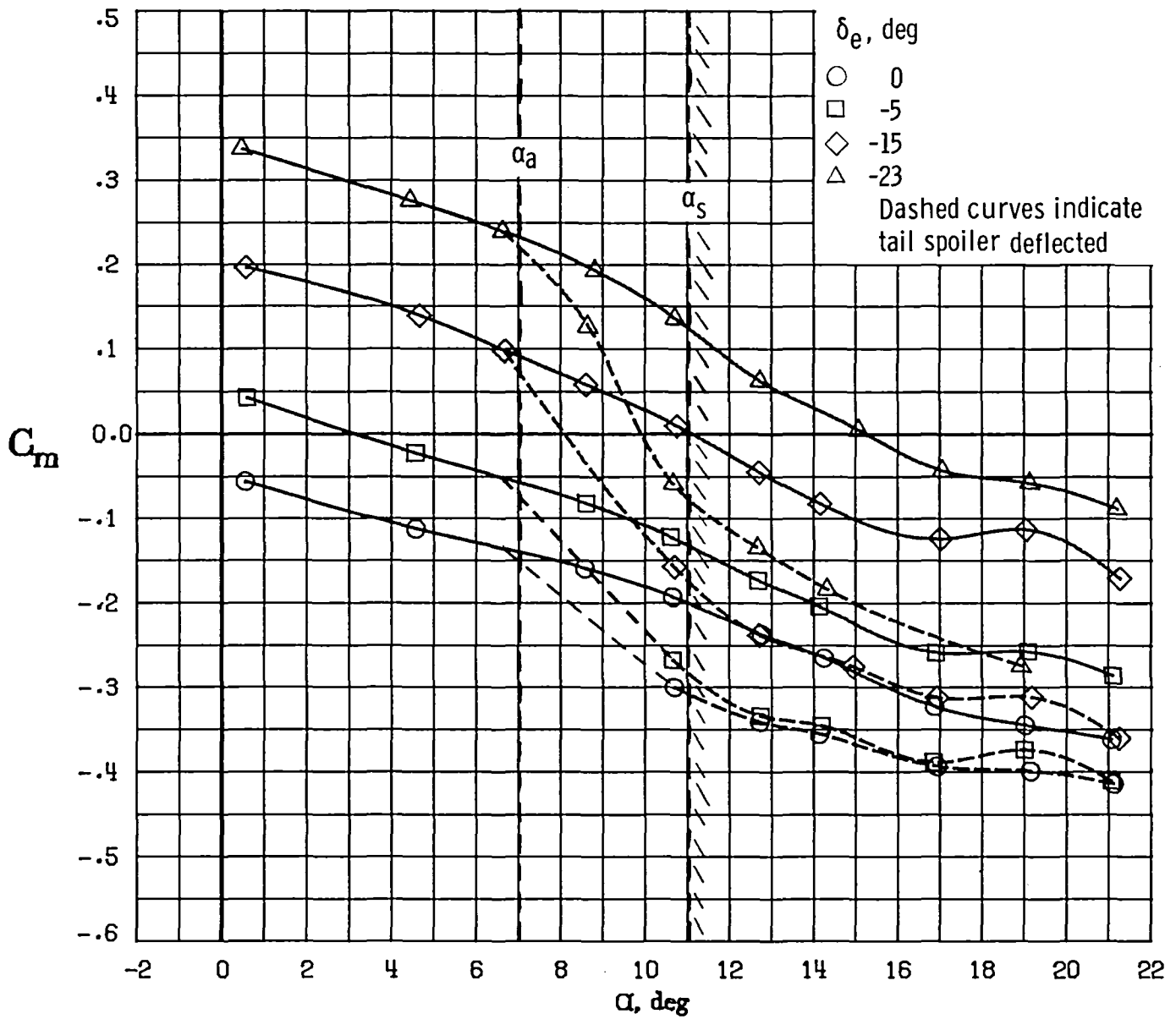
(b) Go-around condition. $C_{T_1} = 0.25$; $\delta_f = 30^\circ$.

Figure 17.- Concluded.



(a) Aft c.g., go-around condition. c.g. = $0.271\bar{c}$; $C_{T_1} = 0.25$; $\delta_f = 30^\circ$.

Figure 18.- Effect of tail-spoiler deflection on variation of pitching-moment coefficient with angle of attack.



(b) Forward c.g., cruise condition. c.g. = $0.219\bar{c}$; $C_{T_1} = 0.09$; $\delta_f = 0^\circ$.

Figure 18.- Concluded.

1. Report No. NASA TM-83208		2. Government Accession No.		3. Recipient's Catalog No.	
4. Title and Subtitle WIND-TUNNEL INVESTIGATION OF THE TAIL-SPOILER CONCEPT FOR STALL-PREVENTION ON GENERAL AVIATION AIRPLANES				5. Report Date November 1981	
				6. Performing Organization Code 505-41-13-01	
7. Author(s) Dale R. Satran				8. Performing Organization Report No. L-14703	
9. Performing Organization Name and Address NASA Langley Research Center Hampton, VA 23665				10. Work Unit No.	
				11. Contract or Grant No.	
				13. Type of Report and Period Covered Technical Memorandum	
12. Sponsoring Agency Name and Address National Aeronautics and Space Administration Washington, DC 20546				14. Sponsoring Agency Code	
15. Supplementary Notes					
16. Abstract A wind-tunnel investigation has been conducted in the Langley 30- by 60-Foot Wind Tunnel to determine the longitudinal aerodynamic characteristics of a full-scale, single-engine general aviation airplane equipped with an angle-of-attack limiting concept which used a tail-mounted spoiler for stall prevention. The tail spoiler was deployed as a nonlinear function of changes in angle of attack in a narrow angle-of-attack range immediately preceding the stall angle. Spoiler deployment produced a nose-down moment which limited the nose-up trim capability of the elevator to an angle of attack below the stall angle of the airplane. The tail-spoiler system produced significant increases in longitudinal stability and elevator hinge moments near the stall. The investigation included the effects of power, flaps, and center-of-gravity position.					
17. Key Words (Suggested by Author(s)) General aviation Stability control Stall prevention Tail spoiler				18. Distribution Statement Unclassified - Unlimited Subject Category 01	
19. Security Classif. (of this report) Unclassified	20. Security Classif. (of this page) Unclassified	21. No. of Pages 38	22. Price A03		

National Aeronautics and
Space Administration

Washington, D.C.
20546

Official Business

Penalty for Private Use, \$300

THIRD-CLASS BULK RATE

Postage and Fees Paid
National Aeronautics and
Space Administration
NASA-451



NASA

POSTMASTER: If Undeliverable (Section 158
Postal Manual) Do Not Return
